Insulin–InsR signaling drives multipotent progenitor differentiation toward lymphoid lineages

Pengyan Xia,[1]* Shuo Wang,[1]* Ying Du,[1] Guanling Huang,[1,2] Takashi Satoh,[3] Shizuo Akira,[3] and Zusen Fan[1]

[1]Key Laboratory of Infection and Immunity of CAS, Institute of Biophysics, Chinese Academy of Sciences, Beijing 100101, China
[2]University of Chinese Academy of Sciences, Beijing 100049, China
[3]Department of Host Defense, Research Institute for Microbial Diseases (RIMD), Osaka University, Suita, Osaka 565-0871, Japan

The lineage commitment of HSCs generates balanced myeloid and lymphoid populations in hematopoiesis. However, the underlying mechanisms that control this process remain largely unknown. Here, we show that insulin–insulin receptor (InsR) signaling is required for lineage commitment of multipotent progenitors (MPPs). Deletion of Insr in murine bone marrow causes skewed differentiation of MPPs to myeloid cells. mTOR acts as a downstream effector that modulates MPP differentiation. mTOR activates Stat3 by phosphorylation at serine 727 under insulin stimulation, which binds to the promoter of Ikaros, leading to its transcription priming. Our findings reveal that the insulin–InsR signaling drives MPP differentiation into lymphoid lineages in early lymphopoiesis, which is essential for maintaining a balanced immune system for an individual organism.

Hematopoiesis is the process of producing all components of the blood system from hematopoietic stem cells (HSCs; Naik et al., 2013; Mendelson and Frenette, 2014; Walter et al., 2015). HSCs are quiescent, self-renewable progenitor cells that need contact with stromal cells to keep their self-renewal property (Morrison and Scadden, 2014; Schepers et al., 2015). Once HSCs sense signals for differentiation, asymmetry division occurs and HSCs that lose contact with stromal cells are doomed to differentiate into early lineage-restricted progenitors (Will et al., 2013; Tamplin et al., 2015). Many signature markers of the oligopotent progenitors have been defined, and these progenitor populations can be successfully isolated from LSKs ($Lin^-Sca\text{-}1^+c\text{-}Kit^+$ cells) for further study (Kfoury et al., 2014; Riddell et al., 2014). Flt3 (also known as Flk2) plays a critical role in lymphoid lineage specification. Multipotent progenitors (MPPs) can generate either granulocyte/monocyte progenitors (GMPs) or common lymphoid progenitors (CLPs; Kondo, 2010). GMPs generate myeloid cells, accompanied by the loss of lymphoid potential (Iwasaki and Akashi, 2007), whereas CLPs give rise to all lymphoid cells, coupled with the loss of myeloid potential (Adolfsson et al., 2005). Thus, these two downstream progenitors govern the myeloid and lymphoid developmental programs independently (Iwasaki and Akashi, 2007). However, the molecular mechanisms regulating MPP fate decisions between GMPs and CLPs remain largely unknown.

Insulin, as the primary anabolic hormone, modulates a variety of physiological processes, including growth, differentiation, apoptosis, and synthesis and breakdown of lipid, protein, and glucose (Samuel and Shulman, 2012). Insulin binds to its insulin receptor (InsR) to activate the receptor intrinsic tyrosine kinase, leading to activation of the PI3K–Akt pathway (Taguchi and White, 2008; Hers et al., 2011). Insulin signaling is indispensable for glucose metabolism in cells of the muscle and adipose tissues (Taguchi and White, 2008; Bogan, 2012). A previous study reported that insulin signaling in *Drosophila melanogaster* controls the maintenance of hematopoietic progenitors (Shim et al., 2012). Suppression of insulin signaling leads to skewing differentiation of progenitor cells to myeloid cells (Shim et al., 2012). It has been reported that diabetic patients display increased numbers of leukocytes, but decreased numbers of lymphocytes (Otton et al., 2004). Moreover, due to immune dysfunction, diabetic patients are susceptible to microbial infection (Cani et al., 2007; Khan et al., 2014). However, how the insulin signaling regulates the HSC fate decision in mammalian hematopoiesis is still elusive.

Accumulating evidence has shown that transcriptional regulation plays a critical role in differentiation commitment of HSCs into consequent early MPPs (Iwasaki and Akashi, 2007; Rossi et al., 2012). Before lineage-specific genes are fully expressed, chromatins of progenitors must be maintained in a wide-open state that could be accessible for transcription machinery (Akashi et al., 2003; Iwasaki and Akashi, 2007). Several transcription factors have been involved in the fate determination of MPPs to the following progenitors, such as GMPs and CLPs (Uhmann et al., 2007; Laurenti et al., 2013;

*P. Xia and S. Wang contributed equally to this paper.

Correspondence to Zusen Fan: fanz@moon.ibp.ac.cn

Abbreviations used: CFC, colony forming cell; CLP, common lymphoid progenitor; GMP, granulocyte/monocyte progenitor; LT-CIC, long-term culture initiating cell; LT-HSC, long-term hematopoietic stem cell; MPP, multipotent progenitor; mTOR, mechanistic target of rapamycin; ST-HSC, short-term hematopoietic stem cell.

The Rockefeller University Press $30.00
J. Exp. Med. 2015 Vol. 212 No. 13 2305–2321
www.jem.org/cgi/doi/10.1084/jem.20150618

Will et al., 2013). The Ikaros family of transcription factors, characterized by their zinc finger domains, is composed of Ikaros, Aiolos, Helios, Eos, and Pegasus proteins (Georgopoulos, 2002). Ikaros is highly expressed in the lymphoid-related subset. *Ikaros*-deficient mice have severe defects in the formation of fetal and adult lymphocytes (Urban and Winandy, 2004; Yoshida et al., 2006). Of note, the cell number of myeloid cells is increased in *Ikaros* knockout mice (Iwasaki and Akashi, 2007), suggesting that Ikaros plays a central role in the hematopoietic lineage decision. It has been reported that Stat3 plays a pivotal role in the maintenance of pluripotency of embryonic stem cells and self-renewal of HSCs (Raz et al., 1999; Chung et al., 2006). A recent study showed that mice with Stat3 conditional deletion in the hematopoietic system display a shifted lymphoid/myeloid ratio (Mantel et al., 2012), suggesting that Stat3 may also be implicated in hematopoietic lineage specification. Here, we show that InsR is constitutively expressed in multipotent hematopoietic progenitors. *Insr* deficiency leads to differentiation of MPPs into myeloid cells accompanied by reduced lymphoid cells. The insulin–InsR signaling is required for lymphoid lineage specification in early lymphopoiesis.

RESULTS

Insr knockout mice increase myeloid cells but decrease lymphoid cells

To explore the role of insulin signaling in hematopoiesis, we first checked expression levels of InsR in the hematopoietic system. InsR was constitutively expressed in all the hematopoietic progenitors and had a higher expression level in MPPs than other populations (Fig. 1 A and Fig. S1 A). The expression levels of InsR in LSKs were further validated by confocal microscopy (Fig. 1 B). We then generated $MxCre^{+}$;$Insr^{flox/flox}$ mice by crossing *MxCre* mice with $Insr^{flox/flox}$ mice (Brüning et al., 1998). After injecting poly(I:C) three times in 5 d to induce expression of the Cre recombinase, Insr was deleted thoroughly in the BM of Insr conditional knockout mice (Fig. 1 C; hereafter called $Insr^{+/+}$ for control mice and $Insr^{-/-}$ for KO mice). $Insr^{-/-}$ mice showed no abnormal phenotypes, and $Insr^{-/-}$ body weights were similar to their littermate $Insr^{+/+}$ control mice. Importantly, $Insr^{-/-}$ mice displayed enlarged spleens (Fig. 1 D), with expansion of spaces between lymphoid follicles (Fig. 1 E). Moreover, $Insr^{-/-}$ spleens had an expansion of myeloid cells but a reduction of lymphoid cells (Fig. 1 F). The skewing myeloid/lymphoid ratio was also observed in BM examined by flow cytometry using markers for myeloid cells (Fig. 1 G) and lymphoid cells (Fig. 1 H).

Dynamic analysis of BM cells showed that myeloid cells in BM increased gradually after *Insr* deletion (Fig. 1 I), accompanied by declined lymphoid cells (Fig. 1 J). Moreover, mature cells positive for specific myeloid markers were significantly increased (Fig. 1 K), whereas B cells were markedly decreased in *Insr* KO mice (Fig. 1 K). When we checked peripheral blood compositions, we found that myeloid-derived cells were dramatically increased, but lymphoid-derived cells were decreased (Table 1 and Fig. 1 L). Additionally, absolute numbers of lymphoid cells were markedly declined in *Insr* KO BM 16 wk after *Insr* deletion (Fig. 1 M). Collectively, these results indicate that *Insr* deficiency increases myeloid cells but reduces lymphoid cells.

Insr-deficient LSKs tend to differentiate into myeloid cells but not lymphoid cells

We stained $Insr^{+/+}$ and $Insr^{-/-}$ BM cells with several cellular surface markers that could distinguish between self-renewable stem cells and differentiated progenitor cells (Fig. 2 A and Fig. S1 B). As expected, progenitors for granulocyte/monocyte progenitors (GMPs) were remarkably increased in $Insr^{-/-}$ BM cells (Fig. 2 B), whereas CLPs were decreased. However, cell numbers of self-renewable hematopoietic stem cells (HSCs) and MPPs in the LSK population were unchanged after *Insr* deletion (Fig. 2 B). We then intraperitoneally injected BrdU (7.5 mg/kg) into $Insr^{+/+}$ and $Insr^{-/-}$ mice for 18 h, and then examined BrdU incorporation in isolated GMPs and CLPs. We found the percentages of BrdU-positive cells were comparable between $Insr^{+/+}$ and $Insr^{-/-}$ cells (Fig. 2 C). Moreover, the S/G2/M state was also comparable between $Insr^{+/+}$ and $Insr^{-/-}$ cells through cell cycle analysis with Hoechst 33342 and pyronin Y staining (Fig. 2 D). Finally, we checked the activation state of caspase-3, an early marker of apoptosis. We found that the apoptotic cells were comparable between $Insr^{+/+}$ and $Insr^{-/-}$ cells (Fig. 2 E). These results suggest that the shifted ratio of the GMPs and CLPs might be caused by differentiation commitment of the LSK population.

Self-renewal is essential for HSCs to maintain their population long term, and altered self-renewal activity can affect the numbers of downstream populations (Riddell et al., 2014; Tamplin et al., 2015). To test whether the self-renewal property was changed in $Insr^{-/-}$ LSK cells, we used a long-term culture initiating cell (LT-CIC) assay to detect the long-term self-renewal ability of *Insr* deficient cells. Consistent with the unchanged composition of LSKs determined by flow cytometry, percentages of colony-forming cells (CFCs) were comparable between $Insr^{-/-}$ and $Insr^{+/+}$ LSKs (Fig. 2 F), indicating that the skewed myeloid/lymphoid ratio in $Insr^{-/-}$ mice was not caused by abnormality in self-renewal of LSKs. Moreover, when we sequentially transplanted $Insr^{+/+}$ and $Insr^{-/-}$ LSKs into recipient mice, similar numbers of reconstituted LSKs were observed (Fig. 2 G), suggesting that the self-renewal capacity of LSKs was not affected by *Insr* deletion. We then used an in vitro assay to test the differentiation potential of $Insr^{-/-}$ LSKs. $Insr^{-/-}$ LSKs exhibited enhanced differentiation potential to myeloid cells in CFC assays (Fig. 2 H), but decreased lymphoid differentiation potential when co-cultured with OP9 cells (Fig. 2 I). However, the differentiation potential toward erythrocytes was not changed after Insr depletion (Fig. 2 J). These data suggest that Insr deletion biases LSKs to differentiate into myeloid cells.

To further verify that the biased differentiation potential of $Insr^{-/-}$ LSKs was intrinsic, we transplanted BM cells

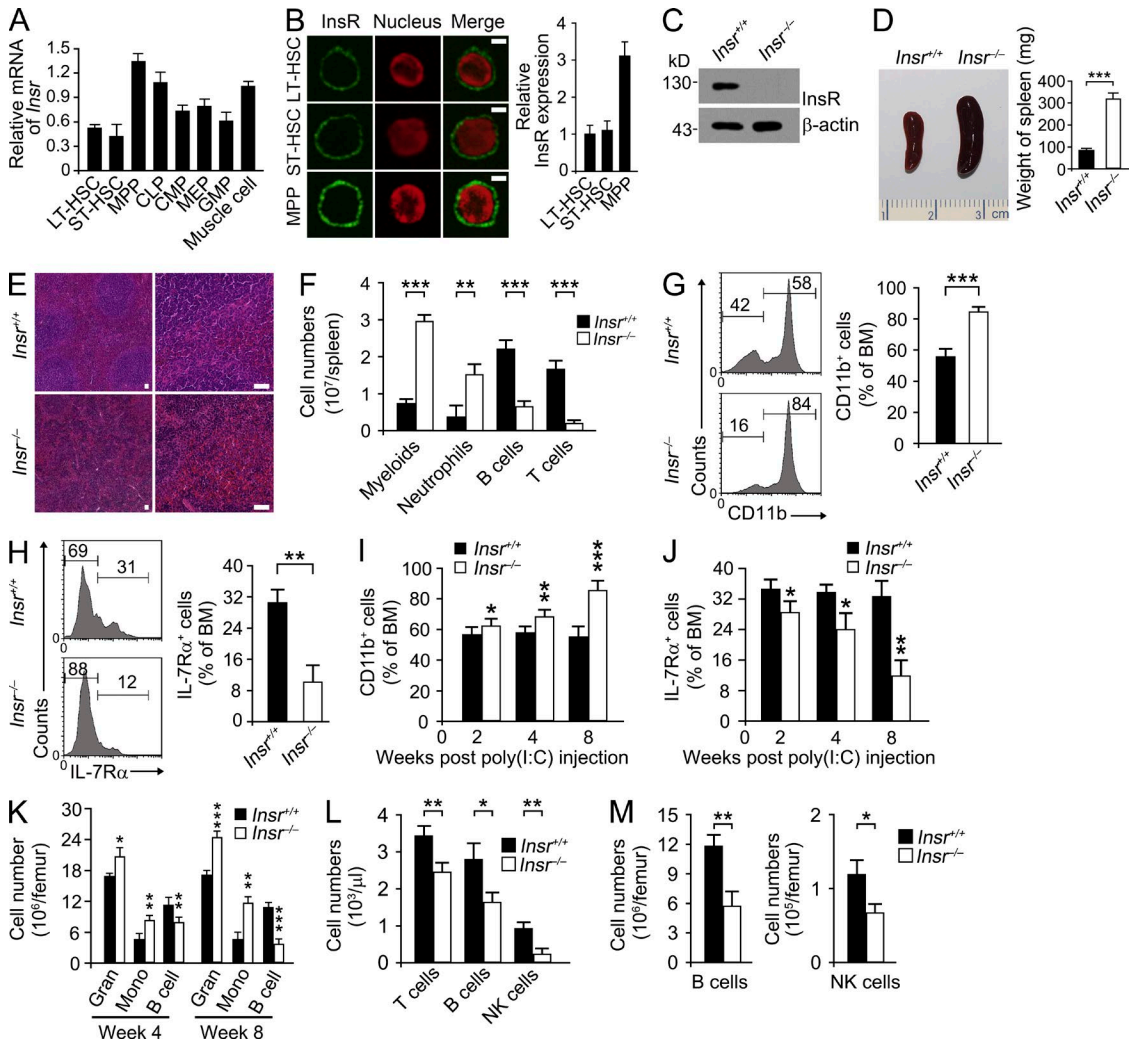

Figure 1. ***Insr* knockout mice have more myeloid cells but fewer lymphoid cells.** (A) Cells from BM were sorted through flow cytometry using the following markers: Lin$^-$ IL-7Rα$^-$ Sca-1$^+$ c-Kit$^+$ CD150$^+$ Flk2$^-$ CD48$^-$ for LT-HSCs, Lin$^-$ IL-7Rα$^-$ Sca-1$^+$ c-Kit$^+$ CD150$^-$ Flk2$^-$ CD48$^-$ for ST-HSCs, Lin$^-$ IL-7Rα$^-$ Sca-1$^+$ c-Kit$^+$ CD150$^-$ Flk2$^+$ for MPPs, Lin$^-$ IL-7Rα$^+$ c-Kit^{low} Sca-1^{low} for CLPs, Lin$^-$ IL-7Rα$^-$ Sca-1$^-$ c-Kit$^+$CD34$^+$ FcγRII/III$^-$ for common myeloid progenitors, Lin$^-$ IL-7Rα$^-$ Sca-1$^-$ c-Kit$^+$ CD34$^-$ FcγRII/III$^-$ for MEPs, and Lin$^-$ IL-7Rα$^-$ Sca-1$^-$ c-Kit$^+$ CD34$^+$ FcγRII/III$^+$ for GMPs. Insr was examined in sorted cell populations through RT-PCR. mRNA levels were first standardized to β-actin, and are shown relative to that of muscle cells. (B) The indicated cells were stained with anti-InsR antibody (green) and counterstained with propidium iodide (PI; red) for nuclei, followed by confocal microscopy. Fluorescence intensity of InsR was calculated and shown as relative to that of LT-HSCs. (C) InsR expression was examined in BM cells from *Insr*$^{+/+}$ or *Insr*$^{-/-}$ mice using antibody against InsR-β. β-actin was probed as a loading control. (D) *MxCre*$^-$;*Insr*$^{flox/flox}$ or *MxCre*$^+$;*Insr*$^{flox/flox}$ mice were intraperitoneally injected with 300 µg poly(I:C) every other day for a total of three times. 8 wk after the last poly(I:C) injection, spleens were examined and the weight was shown in the right panel. (E) Hematoxylin and eosin staining of spleens 8 wk after the last poly(I:C) injection. (F) Leukocytes in spleens analyzed by flow cytometry at 8 wk after poly(I:C) administration. The following surface markers were used: CD11b for myeloid cells, CD11b and Gr1 for neutrophils, B220 for B cells, and CD3ε for T cells. For D–F, 7 *Insr*$^{+/+}$ mice and 9 *Insr*$^{-/-}$ mice were used. (G) BM cells from *Insr*$^{+/+}$ and *Insr*$^{-/-}$ mice were stained with CD11b for myeloid cells. (right) Percentages of CD11b-positive cells. (H) BM cells from *Insr*$^{+/+}$ and *Insr*$^{-/-}$ mice were stained with IL-7Rα for lymphoid cells. (right) Percentages of IL-7Rα positive cells. $n = 6$ (G and H). (I and J) Kinetics of myeloid cells (I) and lymphoid cells (J) after poly(I:C) administration. $n = 6$ for each group. (K) Quantitation of BM subsets in *Insr*$^{+/+}$ and *Insr*$^{-/-}$ mice at 4 or 8 wk after poly(I:C) injection. Surface markers were: B220 for B lymphocytes, CD11b$^+$ Gr-1^{high} F4/80$^-$ for granulocytes (Gran), CD11b$^+$ Gr-1$^+$ F4/80$^+$ for monocytes (Mono). $n = 7$ for each group. (L) Numbers of lymphoid cells in peripheral blood of the indicated mice 16 wk after Insr deletion were examined through flow cytometry. Identifying markers were: CD3ε for T cells, B220 for B cells, and NK1.1 for NK cells. (M) Numbers of B cells and NK cells in BM of the indicated mice 16 wk after Insr deletion were calculated through flow cytometry. $n = 5$ (L and M). Bars: (B) 2 µm; (D) 100 µm. Data are shown as means ± SD. *, $P < 0.05$; **, $P < 0.01$; ***, $P < 0.001$. Data presented above were repeated for three times with similar results.

from untreated *MxCre*$^{+}$;*Insr*$^{flox/flox}$ mice to lethally irradiated CD45.1 recipient mice. After successfully reconstituted the recipient BM, poly(I:C) was administrated to induce deletion of the *Insr* gene. The numbers of myeloid and lymphoid cells were examined by flow cytometry. Expectedly, mice reconstituted with *MxCre*$^{+}$;*Insr*$^{flox/flox}$ LSKs had elevated numbers of GMPs, but decreased numbers of CLPs (Fig. 2 K). Subsequently, neutrophils were significantly increased, whereas lymphocytes were decreased in the peripheral blood of *MxCre*$^{+}$;*Insr*$^{flox/flox}$ LSK-reconstituted mice (unpublished data). Moreover, in competitive transplantation experiments, in which 100 *Insr*$^{-/-}$ LT-HSC cells and 3×10^5 CD45.1 BM cells were together transplanted into lethally irradiated CD45.1 mice, the skewed myeloid/lymphoid ratio was still observed (Fig. 2 L). Collectively, our results suggest that Insr-deficient LSKs tend to differentiate into myeloid cells but not lymphoid cells.

Insulin–InsR signaling governs differentiation of LSKs into lymphoid cells

We next wanted to determine whether insulin could regulate LSK differentiation through InsR engagement. We in vitro cultured isolated LSKs with or without insulin. We found that insulin stimulation could cause InsR activation in LSKs (Fig. 3 A). After being cultured in CFC-assay medium for 10 d, MPPs pretreated with insulin had a declined myeloid colony number, whereas cells pretreated without insulin had an increased myeloid colony number (Fig. 3 B). However, insulin challenge had no effect on the differentiation potential of Flk2^{-}LSKs (Fig. 3 B). In contrast, when co-cultured with OP9 for lymphoid differentiation, MPPs pretreated with insulin had more lymphoid cells, whereas MPPs without insulin had fewer lymphoid cells (Fig. 3 C). In addition, insulin incubation did not cause the changes of cell cycle state and apoptotic cell rate in Flk2^{-}LSKs and MPP cells (Fig. 3, D and E). To further determine the physiological role of insulin signal in MPP differentiation, we injected insulin in mice to elevate insulin levels. Importantly, we found that insulin injection caused significantly decreased myeloid progenitor cells (Fig. 3 F), while dramatically increasing lymphoid cells in the BM.

To more clearly delineate the effect of insulin on LSKs in vivo, we monitored the insulin levels of mice during one feeding cycle (Casanova-Acebes et al., 2013). The insulin level was higher at the end of the night (8:00 am), while it was lower at the end of the day (8:00 pm; unpublished data). Consequently, there were more lymphoid cells but fewer myeloid cells at the end of the night compared with those of the day (unpublished data). When mice were starved to decline their circulating insulin levels, we found that starvation-treated mice had more myeloid cells but fewer lymphoid cells than those of control-treated mice (unpublished data), suggesting that the insulin–InsR signaling might be required for the fate decisions of LSKs.

To further determine whether insulin–InsR signaling indeed directs differentiation of LSKs, *Insr*$^{-/-}$ LSKs rescued with InsR were transplanted into lethally irradiated CD45.1-recipient mice (Fig. 3 G). After successfully reconstitution of the recipient BM, mice were injected with insulin to elevate the circulating insulin level. Only mice reconstituted with InsR could rescue *Insr*$^{-/-}$ LSKs for differentiation with insulin stimulation (Fig. 3 H), which was similar to WT LSKs. These data suggest that insulin–InsR signaling affects the fate decision of LSKs. We generated diabetic mice that impaired insulin production (Yan et al., 2015; Fig. 3, I and J). More importantly, these mice had more GMPs but fewer CLPs than those of control mice (Fig. 3 K). Finally, proliferation and apoptosis states of GMPs and CLPs displayed no difference in diabetic mice and WT control mice (Fig. 3, L and M). Notably, IGF1R, the other insulin-binding receptor, was almost undetectable in MPPs (unpublished data). Altogether, the insulin–InsR signaling governs the differentiation of LSKs into lymphoid cell lineages.

It has been reported that HSCs are heterogeneous with myeloid-biased progenitors in CD150^{high}CD34^{-}LSKs (Morita et al., 2010). To test whether the insulin signaling

Table 1. **Hematopoietic parameters**

Parameter	*Insr*$^{+/+}$ (*n* = 12)	*Insr*$^{-/-}$ (*n* = 12)	P-value
Blood			
WBC (×10^3/µl)	12.6 ± 1.5	27.8 ± 3.4	0.00014
RBC (×10^6/µl)	9.3 ± 1.2	10.9 ± 1.5	0.17293
Hemoglobin (g/dl)	16.0 ± 2.3	19.1 ± 1.6	0.09752
Hematocrit (%)	53.0 ± 3.7	56.7 ± 2.8	0.13923
Differential WBC (%)			
Lymphocytes	69.0 ± 4.3	17.8 ± 3.2	8.65×10^{-8}
Neutrophils	24.1 ± 1.6	58.9 ± 5.5	9.12×10^{-7}
Monocytes	3.9 ± 0.7	16.0 ± 0.9	2.68×10^{-10}
Eosinophil	1.5 ± 0.1	8.0 ± 0.6	1.91×10^{-8}
Tissues			
WBC/femur (×10^3/µl)	20.9 ± 1.6	51.8 ± 3.3	3.17×10^{-8}
Spleen (mg)	93.7 ± 5.4	384.4 ± 18.5	1.84×10^{-12}

Differential WBCs were determined by monitoring the morphology of cells stained with May-Grunewald Giemsa. Data are shown as means ± SD.

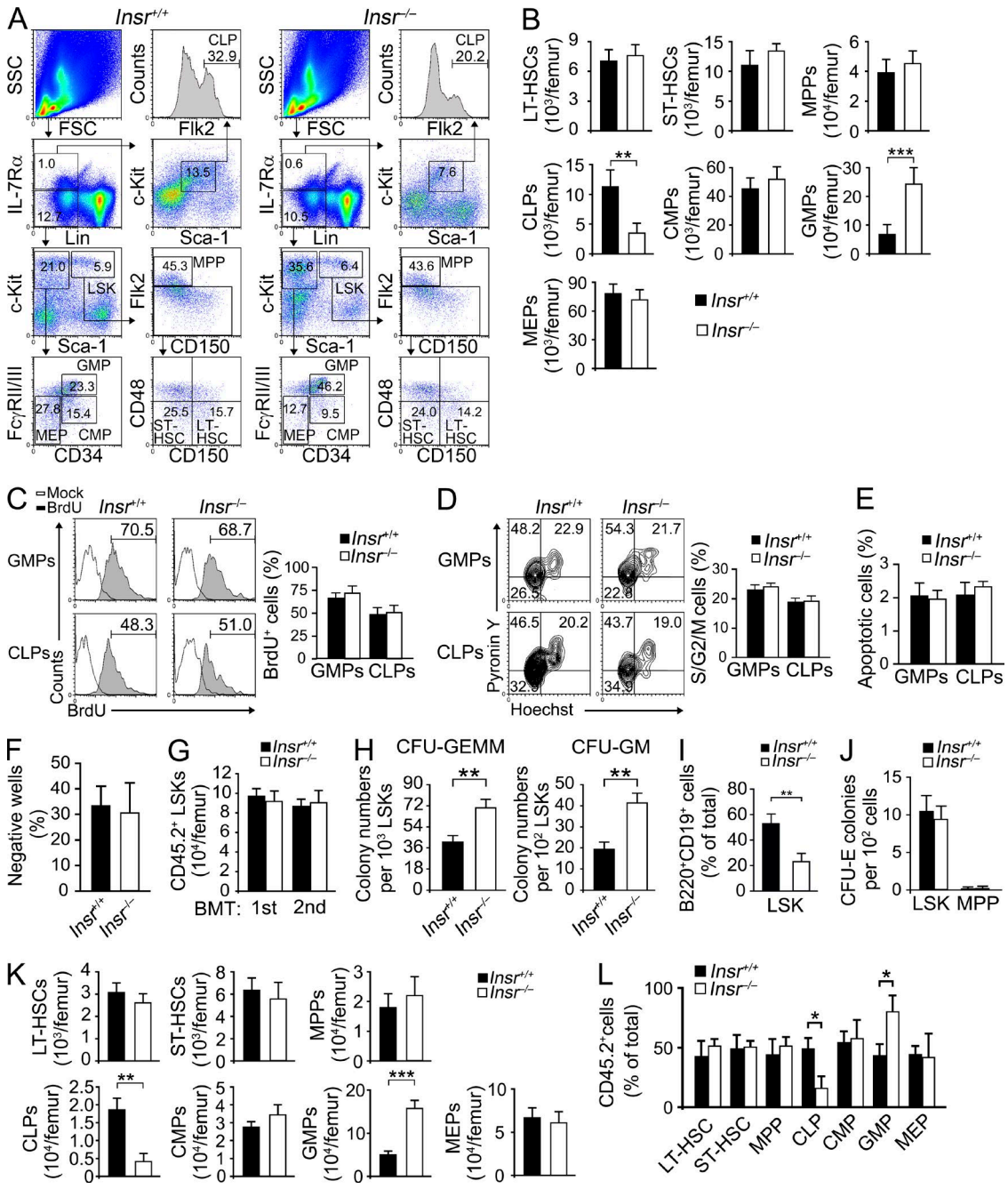

Figure 2. ***Insr*-deficient LSKs tend to differentiate into myeloid cells but not lymphoid cells.** (A) Representative flow cytometry patterns of BM cells prepared from *Insr*$^{+/+}$ and *Insr*$^{-/-}$ mice. The indicated subpopulations were boxed. (B) Quantification of BM cells from *Insr*$^{+/+}$ and *Insr*$^{-/-}$ mice. (A and B) *Insr*$^{+/+}$, $n = 6$; *Insr*$^{-/-}$, $n = 5$. (C) *Insr*$^{+/+}$ and *Insr*$^{-/-}$ mice were intraperitoneally injected with BrdU (7.5 mg/kg) for 18 h, followed by analysis of BM GMPs and CLPs (left). Percentages of BrdU positive cells (right). (D) Cells from *Insr*$^{+/+}$ and *Insr*$^{-/-}$ mice were first stained with Hoechst 33342, and then stained with pyronin Y, followed by flow cytometry (left). Percentages of cells in S/G2/M were calculated (right). (E) *Insr*$^{+/+}$ and *Insr*$^{-/-}$ GMPs and CLPs were permeabilized and stained with antibody against active caspase-3. Cells positive for active caspase-3 were calculated. (F) Long-term culture initiating cell (LT-CIC) assay of LSK cells from *Insr*$^{+/+}$ and *Insr*$^{-/-}$ mice. (G) Equal numbers of *Insr*$^{+/+}$ and *Insr*$^{-/-}$ cells were serially transplanted into lethally irradiated CD45.1 recipients. 16 wk later, repopulation of BM cells were analyzed by flow cytometry for numbers of CD45.2^{+} LSK cells. BMT, BM transplantation. (H) CFC (colony forming cell) assays of LSKs from BM of *Insr*$^{+/+}$ and *Insr*$^{-/-}$ mice. Sorted LSKs were seeded in differentiation medium for 10 d and numbers of colonies were calculated. CFU-GEMM: colony-forming unit-granulocyte, erythrocyte, monocyte/macrophage, megakaryocyte; CFU-GM: colony-forming unit-granulocyte, macrophage. (I) Lymphoid differentiation potential of LSKs from BM of *Insr*$^{+/+}$ and *Insr*$^{-/-}$ mice. 1,000 sorted LSKs were seeded onto OP9 stromal cells supplemented with cytokines needed for lymphoid differentiation and numbers of B220 and CD19 double-positive cells were calculated at the indicated intervals.

is involved in the specification of these cells, we treated $CD150^{high}CD34^{-}$LSKs and $CD150^{neg}CD34^{-}$LSKs with insulin stimulation, and then transplanted these cells together with 3×10^5 CD45.1 BM cells into lethally irradiated mice. Blood constitutions were examined 16 wk later. We observed that insulin stimulation did not alter the myeloid or lymphoid differentiation potential of $CD150^{high}CD34^{-}$LSKs or $CD150^{neg}CD34^{-}$LSKs (Fig. 4, A and B), suggesting that insulin signaling did not affect the differentiation of myeloid-biased progenitors of $CD150^{high}CD34^{-}$LSKs. However, when we transplanted $Insr^{+/+}$ or $Insr^{-/-}$ $CD150^{high}CD34^{-}$LSKs and $CD150^{neg}CD34^{-}$LSKs into recipient mice, we noticed that both $Insr^{-/-}CD150^{high}CD34^{-}$LSKs and $Insr^{-/-}CD150^{neg}CD34^{-}$LSKs promoted myeloid commitment (Fig. 4, C and D), but declined lymphoid differentiation potential. In addition, the overall donor chimerism between these cell populations was similar (Fig. 4, E–H). Moreover, numbers of $CD150^{high}CD34^{-}$LSKs in $Insr^{+/+}$ and $Insr^{-/-}$ mice were comparable (Fig. 4 I). Additionally, numbers of $CD150^{high}$, $CD150^{low}$, and $CD150^{neg}$ $CD34^{-}Flk2^{-}$LSKs in $Insr^{+/+}$ and $Insr^{-/-}$ mice were also comparable (Fig. 4 J). In sum, these data suggest that the insulin signaling is involved in the skewing myeloid/lymphoid differentiation of MPPs, but not in the myeloid-biased HSCs.

Insulin–InsR signaling controls differentiation of LSKs through modulation of Ikaros expression

Lymphopoiesis requires lineage-specific signature genes, such as Ikaros, IL-7R, Lck, and Ly-6D (Akashi et al., 2003; Nodland et al., 2011; Brownlie and Zamoyska, 2013), to direct restricted lineage differentiation. We checked whether insulin initiates expression of these lymphoid signature genes for lymphoid differentiation. Through analyzing enrichment/depletion of lineage signatures (Akashi et al., 2003), we found that lymphoid-related genes tended to be down-regulated, whereas myeloid-related genes were up-regulated in $Insr^{-/-}$ MPPs (Fig. 5, A and B), but not in $Insr^{-/-}$ LT-HSCs or $Insr^{-/-}$ ST-HSCs compared with $Insr^{+/+}$ counterpart populations. Ikaros has been defined as critical for lymphoid differentiation (Iwasaki and Akashi, 2007). Therefore, we focused on the modulation of Ikaros in lymphopoiesis for insulin–InsR signaling. We first examined expression of Ikaros in the BM. Ikaros exhibited the highest expression level in CLPs and a modest level in MPPs (Fig. 5 C), which was consistent with previous reports (Yoshida et al., 2006; Iwasaki and Akashi, 2007). Interestingly, Insr knockout only affected the expression level of Ikaros in MPPs (Fig. 5 C), but remained unchanged in other hematopoietic progenitors.

We then determined Ikaros expression in MPPs under insulin stimulation. We found that insulin promoted the expression of Ikaros in MPPs (Fig. 5 C), but not in LT-HSCs or ST-HSCs. Additionally, *Insr* deficiency could not activate Ikaros expression in MPPs (Fig. 5 C). In parallel, starved mice with a low level of insulin showed reduced expression of Ikaros, and refeeding mice exhibited elevated expression of Ikaros (Fig. 5 D). Moreover, Ikaros was remarkably decreased in MPPs in the starved mice (Fig. 5 E), which was in agreement with the lower insulin level (not depicted). Finally, we found that insulin incubation could promote Ikaros expression in all MPP cells we examined, but not in $Flk2^{-}$LSKs (Fig. 5 F), further validating a restrictive effect of insulin signaling on the Ikaros expression in MPPs.

To further explore the role of Ikaros in the fate decision of MPPs, we reconstituted lethally irradiated mice with either Ikaros-silenced or -overexpressed MPPs. Expectedly, Ikaros knockdown drove MPPs to differentiate into myeloid cells (Fig. 5, G and H), whereas Ikaros overexpression in MPPs led to more lymphoid cells (Fig. 5, I and J), suggesting that Ikaros activation was indispensable for the lymphoid differentiation of MPPs. To further determine the relationship between InsR and Ikaros, we introduced Ikaros to $Insr^{-/-}$ MPPs for rescue experiments (Fig. 5 K). Importantly, $Insr^{-/-}$ MPPs with Ikaros restoration generated fewer myeloid colonies than empty vector-treated $Insr^{-/-}$ MPPs (Fig. 5 L). However, $Insr^{-/-}$ MPPs with Ikaros restoration produced many more lymphoid cells (Fig. 5 M). Additionally, Ikaros restoration was able to rescue colony numbers of $Insr^{-/-}$ MPPs to similar levels with those of $Insr^{+/+}$ MPPs either in a CFC assay or in an OP9 co-culture system (Fig. 5, L and M). These data suggest that Ikaros acts downstream of insulin–InsR signaling to control the fate decision of MPPs.

Insulin–InsR signaling enhances Ikaros expression in MPPs through activation of mTOR

The mechanistic target of rapamycin (mTOR) is a serine/threonine protein kinase that acts as a master regulator of cellular growth and metabolism in response to nutrient and hormonal regulation (Laplante and Sabatini, 2012; Johnson et al., 2013). mTOR was a key regulator downstream of the insulin–InsR signaling pathway (Chi, 2012; Inoki et al., 2012; Powell et al., 2012). To examine whether mTOR is involved in regulation of the expression of Ikaros, we overexpressed mTOR in MPPs and checked the expression level of Ikaros. Interestingly, we found that mTOR overexpression in MPPs dramatically increased the expression level of Ikaros upon insulin stimulation (Fig. 6, A and B). However, without insulin

(J) CFC assays of LSKs and MPPs from BM of $Insr^{+/+}$ and $Insr^{-/-}$ mice. CFU-E, colony-forming unit erythroid. (C–J) $n = 6$. (K) Lethally irradiated CD45.1 mice were transplanted with BM cells from $MxCre^{-};Insr^{flox/flox}$ or $MxCre^{+};Insr^{flox/flox}$ mice. Reconstituted CD45.1 mice were then administrated with poly(I:C) and analyzed by flow cytometry 8 wk after *Insr* deletion. $n = 7$ per strain. (L) 100 $Insr^{+/+}$ and $Insr^{-/-}$ LT-HSCs were cotransplanted with 3×10^5 CD45.1 BM cells into lethally irradiated CD45.1 mice, followed by progenitor cell examination in reconstituted BM 8 wk later. $n = 8$ per strain. Data are shown as means ± SD. *, $P < 0.05$; **, $P < 0.01$; ***, $P < 0.001$. Data represent at least three separate experiments.

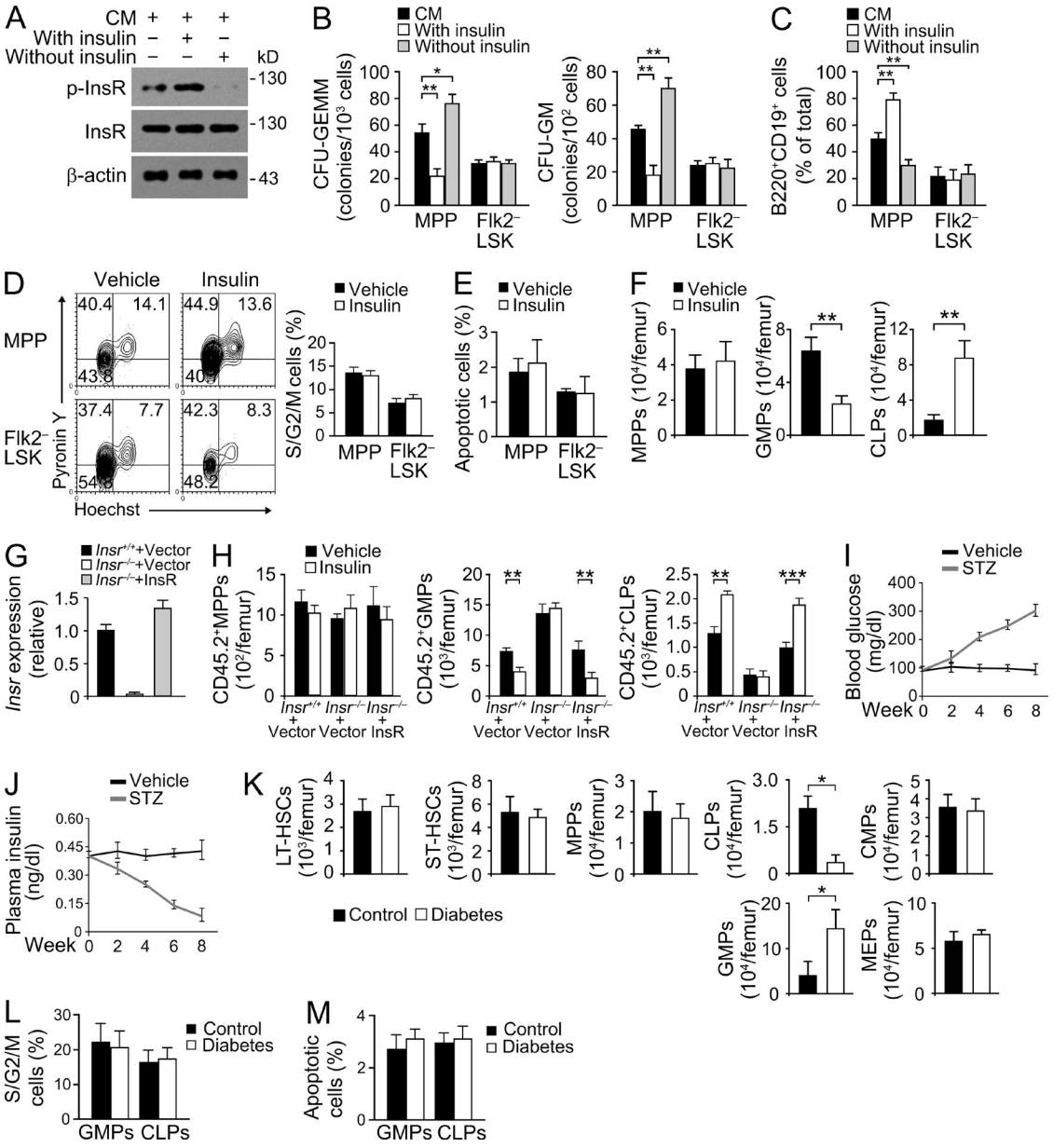

Figure 3. **Insulin signaling drives differentiation of LSKs into lymphoid cells.** (A) Sorted WT LSKs were cultured in StemPro-34 medium as described in Materials and methods. For insulin stimulation (With insulin), insulin was added to the medium to a final concentration of 200 nM for 18 h. For insulin depletion (Without insulin), anti-insulin antibody was added to the medium to reach 1 µg/ml for 18 h. Phosphorylation of Insr was detected using antibody against phospho-insulin receptor β (Tyr1150/1151). CM, culture medium. (B) CFC assays of Flk2⁻LSKs and MPPs pretreated with or without insulin. Sorted cells pretreated with or without 200 nM insulin for 18 h in StemPro-34 medium were seeded in differentiation medium for 10 d and numbers of colonies were calculated. (C) Lymphoid differentiation potential of Flk2⁻LSKs and MPPs cultured with or without insulin. 1,000 sorted cells, pretreated with or without insulin, were seeded onto OP9 stromal cells (see Materials and methods) and numbers of B220⁺CD19⁺ cells were calculated at the indicated intervals. (D) Cells treated with or without insulin were first stained with Hoechst 33342 and then stained with pyronin Y, followed by flow cytometry (left). Percentages of cells in S/G2/M (right). (E) Flk2⁻LSKs and MPPs treated with or without insulin were permeabilized and stained with antibody against active caspase-3. Cells positive for active caspase-3 were calculated. (D and E) $n = 6$. (F) 5 IU/kg of insulin or PBS (Vehicle) were injected into mice through a tail vein at the end of the day (8:00 p.m.) six times, and the BM was analyzed for the indicated populations in the morning of the day (8:00 am) after last insulin injection. $n = 8$ per group. (G and H) Insr reintroduction rescues the phenotype observed in *Insr*$^{-/-}$ mice. LSKs from *Insr*$^{+/+}$ or *Insr*$^{-/-}$ mice were infected with lentivirus encoding the indicated plasmids (G) and then transplanted to lethally irradiated CD45.1 mice together with 3×10^5 CD45.1 BM cells. 16 wk later, numbers of the indicated CD45.2-positive cells were calculated by flow cytometry (H). $n = 6$ per group. (I and J) Generation of diabetic mice. Mice were injected with streptozotocin (STZ; 80 mg/kg i.p. for four consecutive days; vehicle, 0.1 M sodium citrate, pH 4.5) to induce diabetes. The indicated mice were examined for the levels of blood glucose (I) and plasma insulin (J) at the indicated intervals. (K) Diabetic mice induced by STZ were examined for the indicated cell

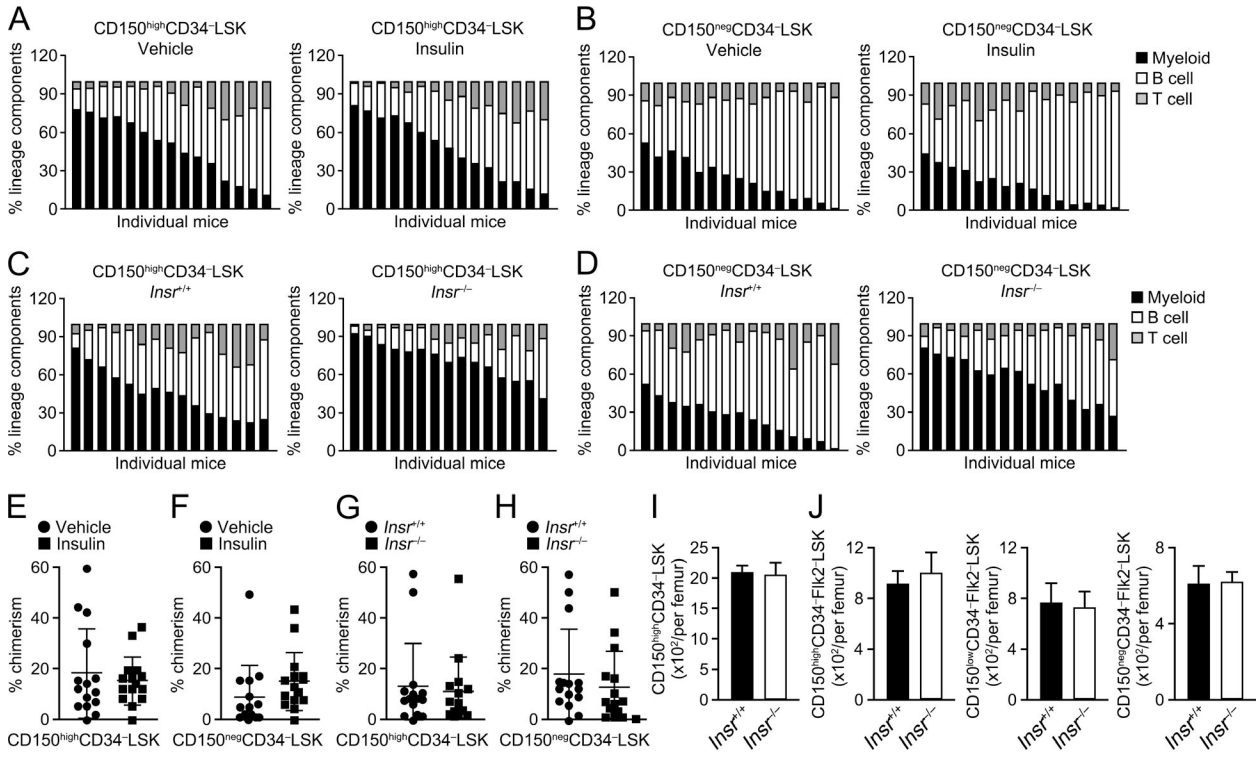

Figure 4. **Insulin–InsR signaling skews myeloid/lymphoid differentiation, but not myeloid-biased HSCs.** (A and B) 10 $CD150^{high}CD34^{-}$LSK or $CD150^{neg}CD34^{-}$LSK cells pretreated with 200 nM insulin for 18 h were transplanted together with 3×10^5 CD45.1 BM cells into lethally irradiated mice, followed by examination of blood constitutions 16 wk later. Relative myeloid, B cell, and T cell compositions were presented. (C and D) 10 $CD150^{high}CD34^{-}$LSK or $CD150^{neg}CD34^{-}$LSK cells from $Insr^{+/+}$ and $Insr^{-/-}$ mice were transplanted together with 3×10^5 CD45.1 BM cells into lethally irradiated mice, and assessed as in A. (E–H) 10 of the indicated cells were transplanted together with 3×10^5 CD45.1 BM cells into lethally irradiated mice, followed by donor chimerism examination 16 wk later. (A–H) $n = 15$. (I) $CD150^{high}CD34^{-}$LSKs were calculated in BM from $Insr^{+/+}$ and $Insr^{-/-}$ mice. (J) $CD34^{-}Flk2^{-}$LSKs were further analyzed by surface marker CD150 and cells with distinct CD150 expression were calculated. (I and J) $n = 6$. Data are shown as means ± SD. Data are from experiments repeated three times with similar results.

stimulation, mTOR overexpression did not enhance Ikaros expression in MPPs. Moreover, we knocked down mTOR expression in MPPs and checked Ikaros expression (Fig. 6 C). We observed that mTOR knockdown remarkably reduced Ikaros expression in MPPs, which was comparable to that of shCtrl MPPs, even with insulin stimulation (Fig. 6 D). These data indicate that insulin–InsR signaling-mediated mTOR activation participates in the transcriptional activation of Ikaros in MPPs.

mTOR functions in two different complexes, mTOR complex 1 (mTORC1) and mTOR complex 2 (mTORC2; Lamming et al., 2012; Bar-Peled et al., 2013). Rapamycin inhibits mTORC1 from suppressing mTOR activity (Yip et al., 2010). Importantly, rapamycin addition could inhibit Ikaros expression in MPPs with insulin stimulation (Fig. 6 E), suggesting that mTORC1 is involved in the expression of Ikaros in MPPs. Moreover, through RT-PCR analysis, mTOR dramatically promoted Ikaros expression (Fig. 6 F), whereas the kinase-dead mTOR mutant (mTOR-KD) had no such activity. These observations verify that mTOR is indeed involved in the transcriptional activation of Ikaros in MPPs. We next determined the effect of rapamycin on MPP differentiation using an in vitro differentiation assay. As expected, MPPs pretreated with rapamycin produced more myeloid cells than vehicle-treated cells (Fig. 6 G); however, rapamycin pretreatment significantly decreased the numbers of lymphoid cells (Fig. 6 H). A reversible inhibitor of PI3Ks, LY294002, acts as an upstream inhibitor of mTOR (Wang et al., 2013). LY294002 could also drive MPPs to myeloid cell differentiation (Fig. 6, I and J). We transplanted shCtrl or mTOR-silenced MPPs

populations through flow cytometry 8 wk after STZ stimulation. (L) Sorted cells were first stained with Hoechst 33342, and then stained with pyronin Y. Percentages of cells in S/G2/M were calculated. (M) GMPs and CLPs from control and diabetic mice were permeabilized and stained with antibody against active caspase-3. Cells positive for active caspase-3 were calculated. (K–M) $n = 7$ per group. Data are shown as means ± SD. *, $P < 0.05$; **, $P < 0.01$; ***, $P < 0.001$. Data are from experiments repeated three times with similar results.

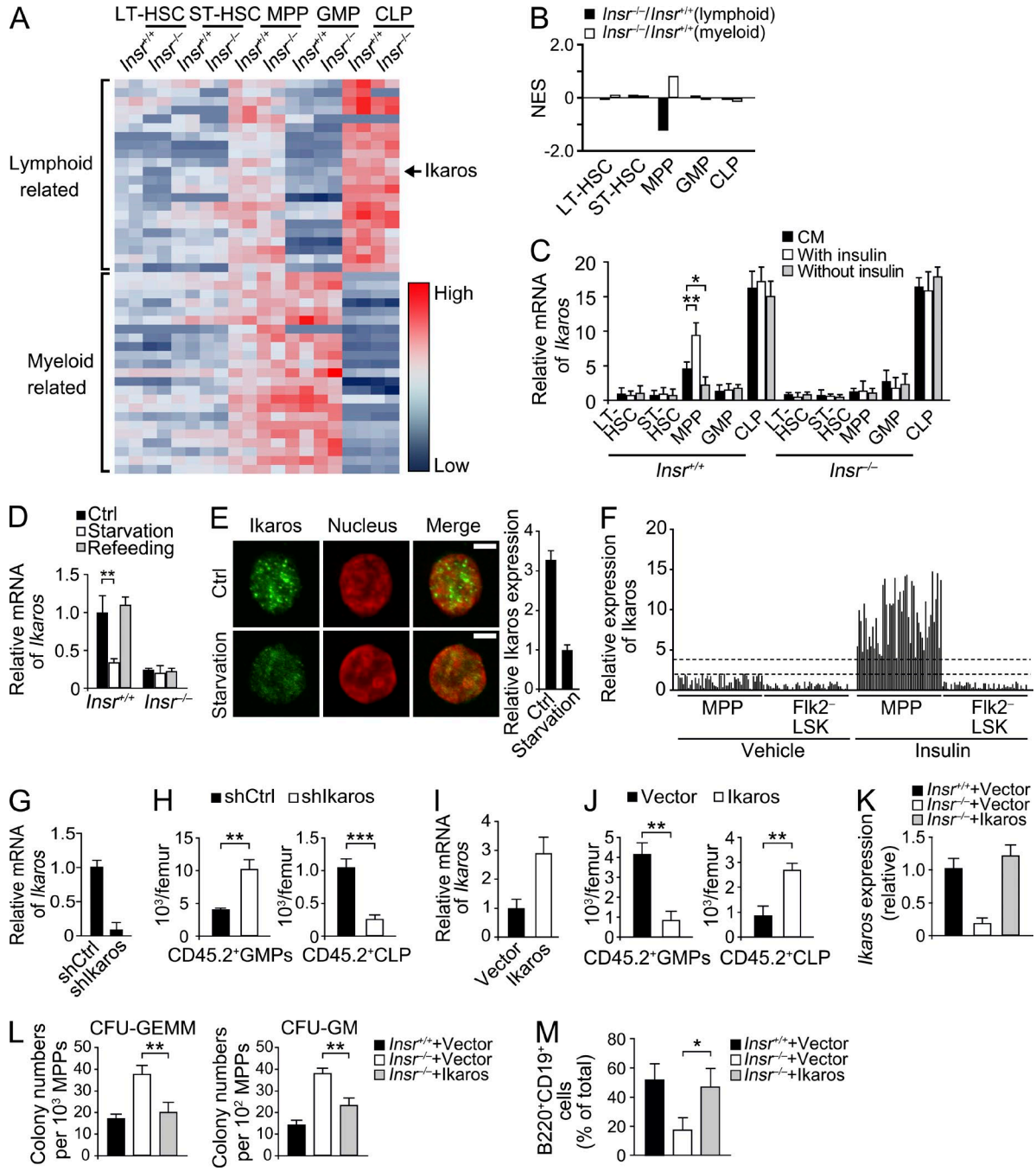

Figure 5. **Insulin–InsR signaling controls the differentiation of LSKs through modulation of Ikaros expression in MPPs.** (A) The indicated genes were examined in sorted cell populations through RT-PCR. mRNA levels were standardized to β-actin. (B) Expression levels of lymphoid and myeloid-related genes obtained above were subjected to gene set enrichment analysis and the normalized enrichment scores (NES) were calculated. (C) Sorted cells were cultured in StemPro-34 medium as described in Materials and methods. mRNA levels were quantified through RT-PCR analysis and results were first standardized to β-actin and then shown relative to that of LT-HSCs of *Insr*$^{+/+}$ mice. CM, culture medium. (D) Mice were supplied with water only from 8:00 a.m. for 48 h, followed by refeeding normally for another 48 h. mRNA levels were analyzed as in C. (E) Sorted MPPs from mice treated with or without starvation for 48 h were stained with anti-Ikaros antibody (green) and counterstained with PI (red) for nuclei. Fluorescence intensity of Ikaros was calculated and shown as relative to that of starvation treated cells. (F) Single cell RT-PCR analysis of Flk2^{-}LSKs and MPPs treated with or without insulin. $n = 6$. (G–J) 5,000 MPPs from WT mice were infected with lentivirus encoding the indicated doxycycline (Dox)-inducible shRNAs (G and H) or overexpressing plasmids (I and J). After incubation with Dox for 36 h (G and H) or 18 h (I and J) to induce the expression of shRNAs or overexpression plasmids, cells with Dox washed off were transplanted to lethally irradiated CD45.1 mice together with 3×10^5 CD45.1 BM cells. 1 wk later, numbers of the indicated CD45.2-positive cells were calculated by flow cytometry. (K and L) Sorted MPPs were infected with lentivirus containing the indicated plasmids for 24 h (K) and then seeded in

into normal or diabetic mice to determine whether mTOR acted downstream of insulin signaling. Intriguingly, we observed that mTOR-silenced MPPs were prone to differentiate into myeloid cells in normal mice (Fig. 6 K). In contrast, this trend did not appear in insulin-suppressed diabetic mice, whose mice had more myeloid cells and fewer lymphoid cells compared with normal mice. In sum, these results suggest that mTOR enhances Ikaros expression that acts downstream of the insulin–InsR signaling in lymphopoiesis.

Stat3 acts as a downstream regulator of insulin–InsR–mTOR signaling to initiate the transcription of Ikaros

To identify the transcription factors that are responsible for Ikaros transcription downstream of insulin–InsR–mTOR signaling in MPPs, we silenced several transcription factors that were known to be regulated by mTOR (Chi, 2012; Powell et al., 2012). Surprisingly, among several factors we checked, only Stat3 knockdown abolished the enhanced expression of Ikaros after insulin stimulation (Fig. 7 A), which was comparable to that of shCtrl-treated cells. Importantly, Stat3 associated with the promoter of Ikaros in MPPs upon insulin stimulation through chromatin immunoprecipitation (ChIP) assays (Fig. 7 B). Moreover, Stat3 could vigorously activate Ikaros expression with insulin administration (Fig. 7, C and D). To further determine the physiological role of Stat3 in Ikaros expression, we generated Stat3 conditional knockout mice in the hematopoietic system. Stat3 was completely deleted in the BM (Fig. 7 E). More importantly, Stat3 deletion impaired the expression of Ikaros upon insulin stimulation (Fig. 7 F). These data suggest that Stat3 binds to the promoter of Ikaros to initiate its expression with insulin stimulation.

Stat3 is activated by a variety of cytokines and growth factors (Casanova et al., 2012). Stat3 is phosphorylated at its two key residues, Tyr705 and Ser727. Ser727 phosphorylation is involved in the modulation of Stat3 activity, whereas Tyr705 phosphorylation participates in its dimerization and activation (Wen et al., 1995; Calò et al., 2003). To determine whether mTOR activates Stat3 upon insulin stimulation in MPPs, we performed immunoblotting with MPP cell lysates obtained from different treatments. Interestingly, we observed that Stat3 was phosphorylated at serine 727 (S727; Fig. 7 G), instead of the canonical site tyrosine 705 (Y705), with insulin stimulation in MPPs. More importantly, rapamycin completely blocked S727 phosphorylation (Fig. 7 G). These data suggest that mTOR acts as an upstream factor to activate Stat3 by its phosphorylation. Furthermore, the serine 727 to alanine mutation (S727A) of Stat3 failed to augment the activation of Ikaros (Fig. 7, H and I), whereas the Y705F Stat3 mutant still augmented Ikaros activation. Additionally, rapamycin addition completely abolished the activation of Ikaros, even when cotransfected with WT Stat3 (Fig. 7 I). Importantly, we observed that Stat3 translocated from the cytoplasm to the nucleus upon insulin stimulation (Fig. 7 J), whereas rapamycin impaired this activity. These results suggest that Stat3 is activated by mTOR with insulin signaling to initiate the transcription of Ikaros.

We found that Stat3 deficiency reduced Ikaros expression upon insulin stimulation (Fig. 7 F). We next detected the differentiation potential of $Stat3^{-/-}$ MPPs. $Stat3^{-/-}$ MPPs produced many more myeloid cells compared with those of WT $Stat3^{+/+}$ cells (Fig. 7 K). In contrast, $Stat3^{-/-}$ MPPs generated fewer lymphoid cells (Fig. 7 L). We then transplanted $Stat3^{-/-}$ or $Stat3^{+/+}$ MPPs into normal or diabetic mice to determine whether Stat3 is the transcription factor downstream of the insulin–InsR signaling. Importantly, we found that $Stat3^{-/-}$ MPPs generated more myeloid cells in normal mice (Fig. 7 M), whereas fewer lymphoid cells. However, in diabetic mice, $Stat3^{-/-}$ MPPs exhibited no such difference. Together, these results indicate that Stat3 acts downstream of insulin–InsR–mTOR signaling to activate the expression of Ikaros in MPPs, leading to lymphoid lineage specification.

DISCUSSION

The lineage commitment of HSCs results in distinct myeloid and lymphoid differentiation pathways, leading to the generation of common myeloid progenitors and CLPs (Iwasaki and Akashi, 2007; Rossi et al., 2012). However, the underlying mechanisms that modulate the lineage specification properties of early progenitors have not been defined yet. In this study, we show that InsR is constitutively expressed in multipotent hematopoietic progenitors. Deletion of InsR in murine BM causes biased differentiation of MPPs toward myeloid cells. Insulin–InsR signaling initiates the expression of Ikaros, which is required for lymphoid differentiation. Without insulin signaling, Ikaros expression is suppressed and MPPs are prone to differentiate into myeloid cells. mTOR acts as a downstream effector that modulates MPP differentiation specification. mTOR activates Stat3 by phosphorylation at serine 727 under insulin stimulation, which translocates to the nucleus of MPPs to bind to the promoter of Ikaros, leading to its transcription priming. Our findings demonstrate that insulin–InsR signaling plays a critical role in governing MPPs toward lymphoid lineages in early lymphopoiesis.

HSCs have an open chromatin structure that allows the transcription of many genes, most of which are myeloid-related (Akashi et al., 2003; Laurenti et al., 2013). Lymphoid-related genes come later during the lineage specification process (Akashi et al., 2003). It is therefore suggested that HSCs are prone to differentiate into myeloid cells and extrinsic signals are required for priming lymphoid lineage

differentiation medium for 10 d and numbers of colonies were calculated (L). (M) 1,000 sorted MPPs transfected with or without Ikaros were seeded onto OP9 stromal cells and numbers of $B220^{+}CD19^{+}$ cells were calculated at the indicated intervals. Bar, 2 µm. Data are shown as means ± SD. *, $P < 0.05$; **, $P < 0.01$; ***, $P < 0.001$. Data are representative of three independent experiments.

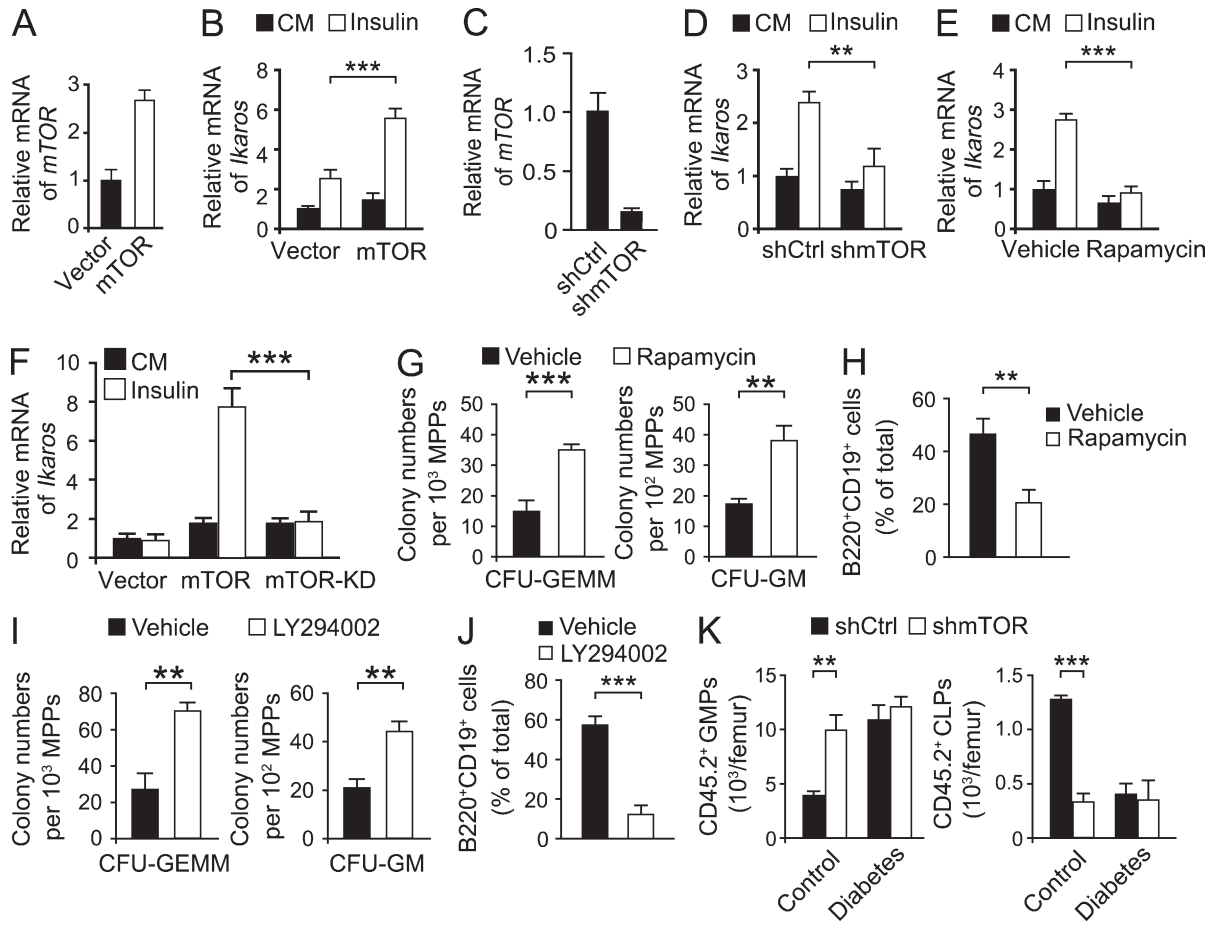

Figure 6. **Insulin–InsR signaling enhances Ikaros expression in MPPs through activation of mTOR.** (A and B) Sorted MPPs infected with lentivirus encoding mTOR or control plasmid (Vector; A) were cultured for 24 h and analyzed by RT-PCR (B) after treatment with or without insulin for 18 h. CM, culture medium. (C and D) Sorted MPPs infected with lentivirus encoding shmTOR or control shRNA (shCtrl; C) were cultured for 36 h and analyzed by RT-PCR (D) after treatment with or without insulin for 18 h. (E) Sorted MPPs treated with rapamycin (100 nM) were cultured with or without insulin for 18 h, followed by RT-PCR. (F) WT MPPs were transfected with WT mTOR or kinase-dead mTOR (mTOR-KD) for 24 h, followed by stimulation with 200 nM insulin for 18 h. (G) Sorted MPPs pretreated as in E were seeded in differentiation medium for 10 d and numbers of colonies were calculated. (H) 1,000 sorted MPPs pretreated with or without 100 nM rapamycin were seeded onto OP9 stromal cells and numbers of $B220^+CD19^+$ cells were calculated at the indicated intervals. (I and J) MPPs were treated with 20 µM LY294002 for 12 h, followed by CFU assays (I) or OP9 co-culture (J). (K) 5,000 sorted CD45.2 MPPs were infected with lentivirus encoding Dox-inducible shCtrl or shmTOR sequences. After incubated with Dox for 36 h to induce the expression of shRNAs, cells with Dox washed off were then transplanted to normal or diabetic CD45.1 mice. 1 wk later, numbers of CD45.2 myeloid progenitors or lymphoid progenitors were calculated in BM by flow cytometry. $n = 7$ for each group. Data are shown as means ± SD. **, $P < 0.01$; ***, $P < 0.001$. Data are from experiments repeated three times with similar results.

commitment. HSCs differentiate to lymphoid-primed MPPs, then to lymphoid-restricted progenitors, accompanied by the loss of erythroid-megakaryocyte and myeloid potential (Adolfsson et al., 2005). More recently, many studies reported the lineage-instructive capacities of several cytokines on hematopoietic stem/progenitor cells. For example, M-CSF directly induces expression of the myeloid master regulator PU.1 to direct myeloid cell-fate specification in mouse HSCs (Mossadegh-Keller et al., 2013). Erythropoietin (Epo) triggers erythroid lineage skewing at all lineage bifurcations between HSCs and erythroid progenitors (Grover et al., 2014). Here, we show that InsR is constitutively expressed in the multipotent hematopoietic progenitors of BM and that extrinsic insulin signaling is required for lymphoid lineage specification in early lymphopoiesis. Notably, we obtained quite high counts of peripheral white blood cells in $Insr^{+/+}$ and $Insr^{-/-}$ mice, which might be caused by a sensitive blood cell counter we used. In reality, *Insr*-deficient mice displayed much higher peripheral white blood cell counts than WT mice. Our study also demonstrates that insulin-suppressed diabetic mice have more myeloid cells and fewer lymphoid cells compared with normal WT mice. A recent study showed that high fat diet–induced obesity produces skewed myeloid progenitors that potentiate generation of macrophages (Singer et al., 2014),

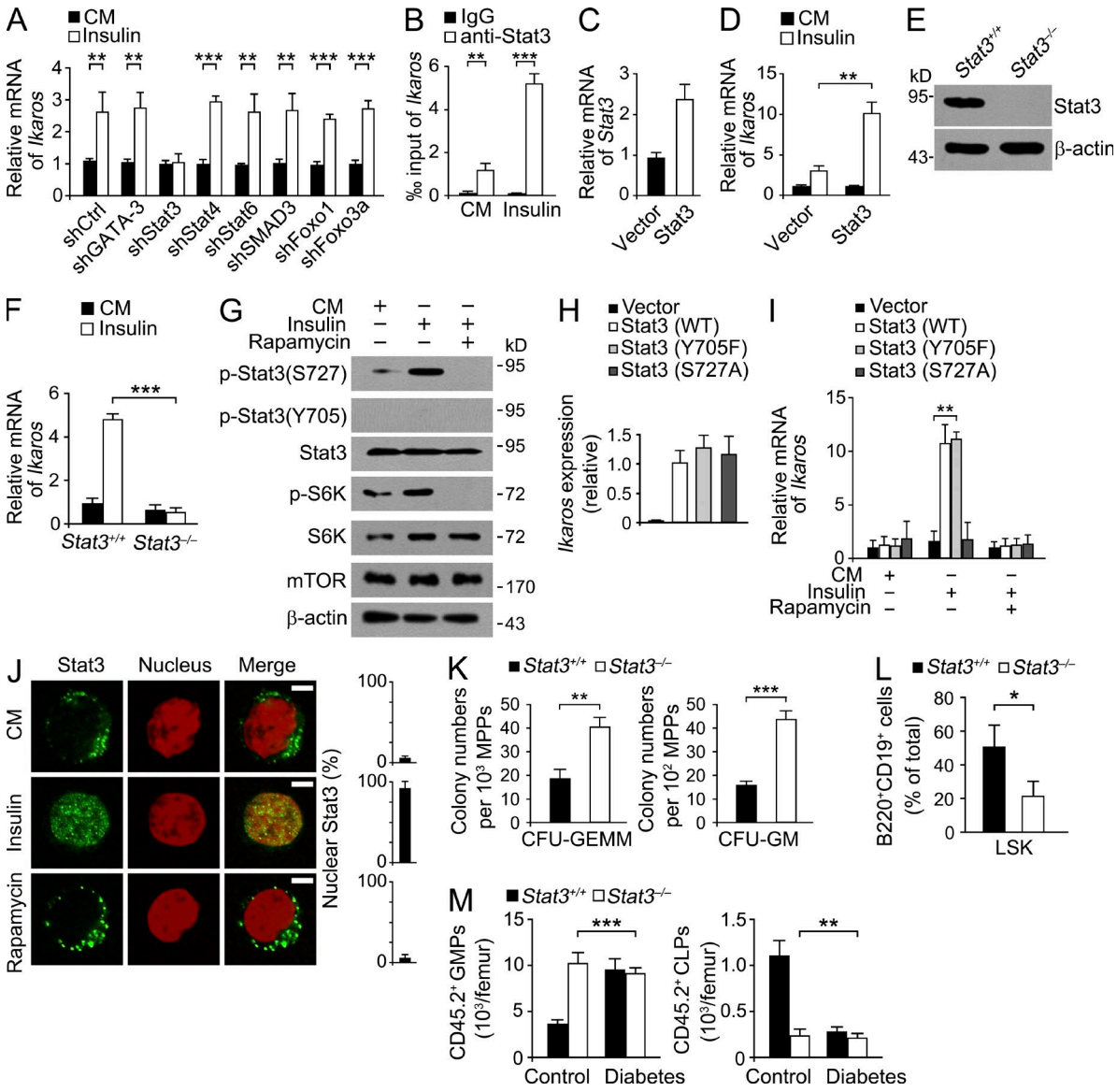

Figure 7. **Stat3 acts downstream of the insulin–InsR–mTOR signaling to up-regulate the expression of Ikaros.** (A) Sorted MPPs infected with lentivirus encoding shRNAs or control shRNA (shCtrl) were cultured for 36 h, followed by analysis of Ikaros expression through RT-PCR. (B) Sorted MPPs cultured with or without insulin (insulin or CM, respectively) for 18 h were lysed for ChIP assays with anti-Stat3 antibody. Immunoprecipitates were examined with RT-PCR. DNA levels were normalized to input. (C and D) WT MPPs were transfected with empty vector or Stat3-vector for 24 h (C), followed by stimulation with 200 nM insulin for 18 h. Ikaros expression was analyzed through RT-PCR (D). (E) *Stat3*$^{flox/flox}$ mice were crossed with *Vav-Cre* mice to generate mice with conditional deletion of Stat3 in the hematopoietic system. Sorted MPPs were examined through immunoblotting. (F) *Stat3*$^{+/+}$ or *Stat3*$^{-/-}$ MPPs were treated with 200 nM insulin for 18 h. Ikaros expression was examined through RT-PCR. (G) Sorted MPPs were cultured in StemPro-34 medium as described in Materials and methods. For mTOR activation (with insulin), insulin was added to the medium to a final concentration of 200 nM for 18 h. For mTOR inhibition (Rapamycin), rapamycin was added to the medium to reach 100 nM for 18 h. Phosphorylation of Stat3 was detected using antibodies against serine 727-phosphorylated Stat3 (p-Stat3 (S727)) or tyrosine 705-phosphorylated Stat3 (p-Stat3 (Y705)). (H and I) *Stat3*$^{-/-}$ MPPs were cotransfected with the indicated plasmids encoding WT Stat3, Y705F-Stat3, or S727A-Stat3 (H), followed by stimulation with 200 nM insulin or 100 nM rapamycin for 18 h. Ikaros expression was examined through RT-PCR (I). (J) Sorted MPPs were treated as in G and stained with antibody against Stat3, followed by confocal microscopy. Fluorescence intensity of nuclear Stat3 was calculated and shown as relative to total Stat3. (K) *Stat3*$^{+/+}$ and *Stat3*$^{-/-}$ MPPs were seeded in differentiation medium for 10 d, and numbers of colonies were calculated. (L) 1000 sorted *Stat3*$^{+/+}$ and *Stat3*$^{-/-}$ MPPs were seeded onto OP9 stromal cells and numbers of B220^{+}CD19^{+} cells were calculated at the indicated intervals. (M) 5,000 sorted CD45.2 *Stat3*$^{+/+}$ and *Stat3*$^{-/-}$ MPPs were transplanted to normal or diabetic CD45.1 mice. 1 wk later, numbers of CD45.2 myeloid progenitors or lymphoid progenitors were calculated in BM by flow cytometry. $n = 7$ for each group. Bar, 2 µm. Data are shown as means ± SD. *, $P < 0.05$; **, $P < 0.01$; ***, $P < 0.001$. Data are from experiments repeated three times with similar results.

augmenting inflammatory responses in metabolic tissues. Interestingly, prolonged fasting can reduce circulating IGF-1 levels in LT-HSCs and niche cells, which promote self-renewal, and lineage-balanced regeneration of HSCs (Cheng et al., 2014). Of note, Ding and Morrison (2013) reported that lymphoid/myeloid-skewed HSCs occupy distinct BM niches (Oguro et al., 2013), suggesting that a specialized microenvironment in which progenitors reside also plays a critical role in hematopoiesis.

The membrane InsR binds to insulin to turn on the PI3K–Akt pathway (Fruman and Rommel, 2014). Akt can phosphorylate to activate mTOR, which is present in two distinct protein complexes: mTORC1 and mTORC2 (Shimobayashi and Hall, 2014). mTORC1 phosphorylates its main effector substrates, eukaryotic translation initiation factor 4E (eIF-4E)–binding protein 1 (4E-BP1) and 70-kD ribosomal S6 protein kinase (S6K), to potentiate protein translation and synthesis. Besides its role in metabolism, mTORC1 is also involved in mitochondrial biosynthesis and autophagy (Cunningham et al., 2007; Yu et al., 2010). Rapamycin binds to FKBP12 by binding to the FRB site on mTOR, which blocks the ability of Raptor to bind to mTOR to inhibit the activity of mTORC1 (Powell et al., 2012). Prolonged treatment with rapamycin for some tissues and cells are able to suppress the mTORC2 activity as well (Sarbassov et al., 2006). In this study, we found that mTOR phosphorylates Stat3 at serine 727, a novel substrate for mTOR, which is indispensable for the transcriptional activation of Ikaros in MPPs. Both mTOR knockdown and rapamycin treatment are able to suppress the expression of Ikaros in MPPs. How mTORC1 and mTORC2 function in early lymphopoiesis remains to be further investigated.

Ikaros plays an essential role in the modulation of lymphoid development and differentiation (Iwasaki and Akashi, 2007). Neonatal Ikaros-null mice appear to be a complete defect in fetal thymocyte development. Adult Ikaros-deficient mice block lymphoid differentiation and exhibit thymocyte development skewed to CD4 T cells (Urban and Winandy, 2004). Interestingly, the numbers of myeloid cells are increased in Ikaros deficient mice. In mature $CD4^+$T cells, Ikaros modulates a variety of processes including Th2 differentiation and cytokine production (Bandyopadhyay et al., 2007; Quirion et al., 2009). In B cells, the transcription factor FoxO1 plays a critical role in Ikaros expression, whereas FoxO1 does not directly initiate Ikaros transcription. However, the transcriptional activation of Ikaros is poorly understood in hematopoietic lineage specification. Here, we show that InsR is highly expressed in hematopoietic progenitors, with the highest level in MPPs. Extrinsic insulin–InsR signaling directly activates Stat3 in MPPs to initiate Ikaros transcription.

Stat3 is well known to maintain the pluripotency of embryonic stem cells under the control of LIF signaling (Yu et al., 2014). Stat3 also participates in sustaining HSC self-renewal (Chung et al., 2006). Mice with Stat3 conditional deletion in the hematopoietic system display increased numbers of myeloid cells and decreased numbers of lymphoid cells, a phenomenon similar to ageing mice (Mantel et al., 2012). Reactive oxygen species (ROS) levels are elevated in HSCs and hematopoietic progenitor cells. Lymphopoietic activity becomes compromised during ageing (Montecino-Rodriguez and Dorshkind, 2006). The earliest lymphoid progenitor pools are declined in aged BM (Miller and Allman, 2005). Senescence may decrease the sensing ability to insulin signaling due to insulin resistance. Disrupted insulin secretion in mouse diabetes models generates more myeloid cells but fewer lymphoid cells, resulting in a skewed myeloid/lymphoid ratio in diabetic mice. It remains to be delineated whether insulin resistance decreases lymphoid lineage differentiation in diabetic patients, which may result in damage of the immune system and increased susceptibility to infections. We expect that our findings will provide useful clues for translational study for diabetic patients. In summary, our observations reveal that insulin–InsR signaling drives MPP differentiation into lymphoid lineages in early lymphopoiesis, which is essential for maintaining a balanced immune system for an individual organism.

MATERIALS AND METHODS

Antibodies and reagents. The following commercial antibodies were used: mouse hematopoietic lineage eFlour 450 cocktail, PerCP-Cy5.5-anti-CD45.1, FITC-anti-CD45.2, Alexa Fluor 700-anti-IL-7Rα, FITC-anti-Ly6A/E (Sca-1), PE-anti-CD117 (c-Kit), APC-eFluor780-anti-CD48, anti-CD3, anti-CD19, FITC-anti-CD11b, PE-anti-Gr1, FITC-anti-B220, Pecy5-anti-CD3ε, APC-anti-Flt3/CD135, anti-F4/80, anti-Gr-1, and anti-CD34 were purchased from eBioscience. PE-cy7-anti-CD150 was obtained from BioLegend. PerCP-Cy5.5–conjugated goat anti–rat IgG and APC-Cy7–conjugated goat anti–rabbit IgG were purchased from Santa Cruz Biotechnology, Inc. Anti–β-actin was from Sigma-Aldrich. Antibodies against Insr-β, phosphorylated Insr-β (Tyr1150/1151), insulin, mTOR, Stat3, S727 phosphorylated Stat3, Y705 phosphorylated Stat3, S6K, and phosphorylated S6K were purchased from Cell Signaling Technology. Donkey anti–rabbit or anti–mouse secondary antibodies conjugated with Alexa Fluor 488, 594, or 405 were purchased from Molecular Probes. HRP-conjugated secondary antibody was obtained from Santa Cruz Biotechnology, Inc. Propidium iodide (PI), Annexin-V, insulin, rapamycin, and streptozotocin (STZ) were purchased from Sigma-Aldrich.

Cell culture. For HSC or MPP culture, cells were cultured in StemPro-34 medium (Invitrogen), containing 4 mM L-glutamine, 100 μg/ml streptomycin, 100 U/ml penicillin, and the following cytokines (all from PeproTech): 10 ng/ml IL-3, 25 ng/ml SCF, 25 ng/ml Ftl-3L, 10 ng/ml GM-CSF, 25 ng/ml IL-11, 4 U/ml Epo, and 25 ng/ml Tpo.

Generation of *Insr* and *Stat3* conditional knockout mice. *Insr*$^{flox/flox}$ mice were purchased from The Jackson Laboratory (B6.129S4(FVB)-Insrtm1Khn/J). *Insr*$^{flox/flox}$ mice were

crossed with *MxCre*$^{+}$ mice to get *MxCre*$^{+}$;*Insr*$^{flox/+}$ mice. The *MxCre*$^{+}$;*Insr*$^{flox/+}$ mice were then crossed with *Insr*$^{flox/flox}$ mice to generate *MxCre*$^{+}$;*Insr*$^{flox/flox}$ mice. *MxCre*$^{+}$;*Insr*$^{flox/flox}$ mice were intraperitoneally injected with 300 µg polyinosine-polycyticylic acid (poly(I:C)) every other day for a total of three times. The recombinant efficacy was examined by Western blotting 5 d after the last poly(I:C) administration using BM cells. *Stat3*$^{flox/flox}$ mice (Takeda et al., 1999) were crossed with *Vav-Cre* mice to generate mice with conditional deletion of Stat3 in the hematopoietic system. Mouse experiments complied with ethical regulations and were approved by the Institutional Animal Care and Use Committees at the Institute of Biophysics, Chinese Academy of Sciences.

Histology. Spleens were fixed in 4% paraformaldehyde (PFA; Sigma-Aldrich) for 12 h. Femurs were fixed in buffer containing 10% formaldehyde for 12 h, and then decalcified in decalcifying buffer (10% EDTA in PBS [wt/wt], pH 7.4) for another 12 h. Fixed tissues were washed twice using 75% ethanol and embedded in paraffin, followed by sectioning and staining with hematoxylin and eosin according to standard laboratory procedures.

Flow cytometry analysis. Flow cytometry was performed as previously described (Xia et al., 2015b). Generally, mice were euthanized and BM cells were flushed out from femur in PBS (phosphate buffered saline) buffer. Spleen cells were generated by mashing the spleen in PBS buffer. Cells were sifted through 50-µm cell strainers after removing red blood cells by suspending cells in ammonium-based red cell lysis buffer. For flow cytometry analysis, cells were stained with fluorophore-conjugated antibodies, followed by detecting or sorting on an Influx cell sorter (BD). Data were analyzed using FlowJo 7.6.1 software (Tree Star).

RNA interference and qRT-PCR. RNA interference was performed as previously described (Xia et al., 2015a). In brief, RNA interference sequences used in this research were designed according to pSUPER system instructions (Oligoengine). H1 promoter and targeting sequences were further cloned to lentivirus vector pSIN-EF2. Lentiviruses were generated by transfecting pSIN-EF2-shRNA and packaging vectors to HEK293T cells, followed by concentration using ultracentrifugation at 50,000 *g*. EML or sorted cells were infected with lentiviruses for 36 h before examination or transplantation. shRNA sequences were: Ikaros, #1, 5′-CAGTGACA CTCCAGATGAA-3′; #2, 5′-GGAAGAATGTGCA GAGGAT-3′; #3: 5′-GAGGCATTCGACTTCCTAA-3′; mTOR, #1, 5′-TGCCAACTACCTTCGAAAC-3′; #2, 5′-AGGAAATGCAGAAGCCTCA-3′; #3, 5′-CCGGCACA CATTTGAAGAA-3′; Stat3, #1, 5′-GAGTCAAGACTGG GCATAT-3′; #2, 5′-CCAGCAATATAGCCGATTC-3′; #3, 5′-CCTCTATCAGCACAACCTT-3′. Total RNA was extracted from sorted cells using TRIzol reagent, and cDNA was reverse-transcribed using Superscript II (Invitrogen). RT-PCR was performed using the following primers: *Ikaros*, forward, 5′-TCGGGAGAGAAAATGAATGG-3′, reverse, 5′-AGGCCGTTCACCAGTATGAC-3′; *Insr*, forward, 5′-AAAGTTTGCCCAACCATCTG-3′, reverse, 5′-GTG AAGGTCTTGGCAGAAGC-3′. Expression was normalized to that of housekeeping gene β-actin. Single-cell RT-PCR was performed as previously described (Luc et al., 2008).

Inducible knockdown and overexpression. Transient knockdown was performed as described previously (Wang et al., 2013). In brief, H1 promoter together with shRNA sequences were first merged with 2 × TetO2 by overlapping PCR and then cloned to pcDNA4/TO/Myc-His B replacing the CMV promoter. For overexpression experiments, cDNA sequences were cloned to the multiple cloning site of pcDNA4/TO/Myc-His B. pcDNA4/TO/Myc-His B was cotransfected with pcDNA6/TR into MPPs by electroporation, followed by addition of doxycycline (1 µg/ml) for 36 h (for knockdown) or 18 h (for overexpression).

Chromatin immunoprecipitation (ChIP). Cells were fixed in 1% formaldehyde for 20 min and then quenched with 0.125 M lysine, followed by swelling in lysis buffer (50 mM Hepes, pH 7.5, 140 mM NaCl, 1% Triton X-100, 0.1% Na-Deoxycholate, and protease inhibitors) for 30 min on ice. Chromatin was sheared to an average length of 400 bp by sonication. After being de-cross-linked by RNase, proteinase K, and heat, input genomic DNA was precipitated with ethanol and quantified in a GeneQuant 100 spectrophotometer (GE Healthcare). Chromatin was precleared with protein A/G-agarose (Santa Cruz Biotechnology, Inc.), followed by incubation with the indicated antibodies at 4°C overnight and further incubation with protein A/G-agarose for 2 h. Beads were washed with washing buffer (10 mM Tris, pH 8.0, 250 mM LiCl, 0.5% NP-40, 0.5% NaDeoxycholate, 1 mM EDTA) three times and eluted with elution buffer (50 mM Tris, pH 8.0, 1% SDS, 10 mM EDTA). Eluates were de-cross-linked by RNase, proteinase K, and heat, and DNA was extracted with phenolchloroform, followed by ethanol precipitation. For each ChIP experiment, 2×10^4 cells were used. 5% of nuclear extracts served as inputs. Immunoprecipitated DNAs were further analyzed by real-time PCR. Signals were normalized to input DNA.

BM transplantation. BM transplantation was performed as described previously (Xia et al., 2014). In brief, donor BM cells were separated as described above and injected alone or with recipient BM cells into lethally irradiated (10 Gy) CD45.1 mice. Reconstituted mice were fed with water containing 1 g/liter ampicillin for 2 wk before switching to regular water. For analysis of peripheral blood cells, blood was obtained from mouse tail vein and stained as described above.

CFC assay. 2×10^4 BM cells were seeded in 35-mm dishes containing IMDM, supplemented with 1.2% methylcellulose

(STEMCELL Technologies), 40 µM 2-mercaptoethanol, 0.5 mM haemin, 30% FBS, 2 mM L-glutamine, 20 ng/ml rmIL-3, 6 U/ml recombinant human EPO, and 20 ng/ml recombinant mouse SCF. Colonies of CFU-GEMM, CFU-GM, and BFU-E were calculated 10 d after incubation at 37°C. LT-CIC assay was performed as previously described (Méndez-Ferrer et al., 2008).

Co-culture with OP9 cells. OP9 cells were cultured in α-MEM supplemented with 20% FBS, 40 µM 2-mercaptoethanol, and 2 mM L-glutamine. For lymphoid differentiation, sorted LSKs or MPPs were plated onto 80% confluent OP9 cells in α-MEM supplemented with 5 ng/ml rmFlt3L and 5 ng/ml rmIL-7 (PeproTech). Cells were stained with anti-CD19 antibody, followed by flow cytometry analysis. Samples were run out to determine the numbers of lymphoid cells (positive for CD19) by flow cytometry.

Generation of experimental mouse models. For circadian rhythm, mice were fed regularly during the night (8:00 p.m. to 8:00 a.m. on the following day) and with water only in the day (8:00 a.m. to 8:00 p.m.). For the starvation/refeeding cycle, mice were supplied with water only from 8:00 a.m. for 48 h, followed by refeeding normally for another 48 h. For generation of diabetic mice, mice were injected with streptozotocin (80 mg/kg i.p. for four consecutive days; vehicle, 0.1 M sodium citrate, pH 4.5) to induce diabetes.

Statistical analysis. Student's *t* test was used as statistical analysis by using Excel (Microsoft; Xia et al., 2013).

Online supplemental material. Fig. S1 shows the gating strategy used in this study. Online supplemental material is available at http://www.jem.org/cgi/content/full/jem.20150618/DC1.

ACKNOWLEDGMENTS

We thank Xuan Yang for protein expression and Yan Teng for technical support.

This work was supported by the National Natural Science Foundation of China (81330047, 31471386, 91419308, and 31300645), 973 Program of the MOST of China (2010CB911902), the Strategic Priority Research Programs of the Chinese Academy of Sciences (XDA01010407), and the China Postdoctoral Science Foundation (2015M571141).

The authors declare no competing financial interests.

Author contributions: P. Xia designed and performed experiments, analyzed data, and wrote the paper; S. Wang performed experiments and analyzed data. G. Huang constructed plasmids; Z. Fan initiated the study, and organized, designed, and wrote the paper.

Submitted: 6 April 2015
Accepted: 9 October 2015

REFERENCES

Adolfsson, J., R. Månsson, N. Buza-Vidas, A. Hultquist, K. Liuba, C.T. Jensen, D. Bryder, L. Yang, O.J. Borge, L.A. Thoren, et al. 2005. Identification of Flt3+ lympho-myeloid stem cells lacking erythro-megakaryocytic potential a revised road map for adult blood lineage commitment. *Cell.* 121:295–306. http://dx.doi.org/10.1016/j.cell.2005.02.013

Akashi, K., X. He, J. Chen, H. Iwasaki, C. Niu, B. Steenhard, J. Zhang, J. Haug, and L. Li. 2003. Transcriptional accessibility for genes of multiple tissues and hematopoietic lineages is hierarchically controlled during early hematopoiesis. *Blood.* 101:383–389. http://dx.doi.org/10.1182/blood-2002-06-1780

Bandyopadhyay, S., M. Duré, M. Paroder, N. Soto-Nieves, I. Puga, and F. Macián. 2007. Interleukin 2 gene transcription is regulated by Ikaros-induced changes in histone acetylation in anergic T cells. *Blood.* 109:2878–2886. http://dx.doi.org/10.1182/blood-2006-07-037754

Bar-Peled, L., L. Chantranupong, A.D. Cherniack, W.W. Chen, K.A. Ottina, B.C. Grabiner, E.D. Spear, S.L. Carter, M. Meyerson, and D.M. Sabatini. 2013. A Tumor suppressor complex with GAP activity for the Rag GTPases that signal amino acid sufficiency to mTORC1. *Science.* 340:1100–1106. http://dx.doi.org/10.1126/science.1232044

Bogan, J.S. 2012. Regulation of glucose transporter translocation in health and diabetes. *Annu. Rev. Biochem.* 81:507–532. http://dx.doi.org/10.1146/annurev-biochem-060109-094246

Brownlie, R.J., and R. Zamoyska. 2013. T cell receptor signalling networks: branched, diversified and bounded. *Nat. Rev. Immunol.* 13:257–269. http://dx.doi.org/10.1038/nri3403

Brüning, J.C., M.D. Michael, J.N. Winnay, T. Hayashi, D. Hörsch, D. Accili, L.J. Goodyear, and C.R. Kahn. 1998. A muscle-specific insulin receptor knockout exhibits features of the metabolic syndrome of NIDDM without altering glucose tolerance. *Mol. Cell.* 2:559–569. http://dx.doi.org/10.1016/S1097-2765(00)80155-0

Calò, V., M. Migliavacca, V. Bazan, M. Macaluso, M. Buscemi, N. Gebbia, and A. Russo. 2003. STAT proteins: from normal control of cellular events to tumorigenesis. *J. Cell. Physiol.* 197:157–168. http://dx.doi.org/10.1002/jcp.10364

Cani, P.D., J. Amar, M.A. Iglesias, M. Poggi, C. Knauf, D. Bastelica, A.M. Neyrinck, F. Fava, K.M. Tuohy, C. Chabo, et al. 2007. Metabolic endotoxemia initiates obesity and insulin resistance. *Diabetes.* 56:1761–1772. http://dx.doi.org/10.2337/db06-1491

Casanova, J.L., S.M. Holland, and L.D. Notarangelo. 2012. Inborn errors of human JAKs and STATs. *Immunity.* 36:515–528. http://dx.doi.org/10.1016/j.immuni.2012.03.016

Casanova-Acebes, M., C. Pitaval, L.A. Weiss, C. Nombela-Arrieta, R. Chèvre, N. A-González, Y. Kunisaki, D. Zhang, N. van Rooijen, L.E. Silberstein, et al. 2013. Rhythmic modulation of the hematopoietic niche through neutrophil clearance. *Cell.* 153:1025–1035. http://dx.doi.org/10.1016/j.cell.2013.04.040

Cheng, C.W., G.B. Adams, L. Perin, M. Wei, X. Zhou, B.S. Lam, S. Da Sacco, M. Mirisola, D.I. Quinn, T.B. Dorff, et al. 2014. Prolonged fasting reduces IGF-1/PKA to promote hematopoietic-stem-cell-based regeneration and reverse immunosuppression. *Cell Stem Cell.* 14:810–823. http://dx.doi.org/10.1016/j.stem.2014.04.014

Chi, H. 2012. Regulation and function of mTOR signalling in T cell fate decisions. *Nat. Rev. Immunol.* 12:325–338. http://dx.doi.org/10.1038/nri3198

Chung, Y.J., B.B. Park, Y.J. Kang, T.M. Kim, C.J. Eaves, and I.H. Oh. 2006. Unique effects of Stat3 on the early phase of hematopoietic stem cell regeneration. *Blood.* 108:1208–1215. http://dx.doi.org/10.1182/blood-2006-01-010199

Cunningham, J.T., J.T. Rodgers, D.H. Arlow, F. Vazquez, V.K. Mootha, and P. Puigserver. 2007. mTOR controls mitochondrial oxidative function through a YY1-PGC-1alpha transcriptional complex. *Nature.* 450:736–740. http://dx.doi.org/10.1038/nature06322

Ding, L., and S.J. Morrison. 2013. Haematopoietic stem cells and early lymphoid progenitors occupy distinct bone marrow niches. *Nature.* 495:231–235. http://dx.doi.org/10.1038/nature11885

Fruman, D.A., and C. Rommel. 2014. PI3K and cancer: lessons, challenges and opportunities. *Nat. Rev. Drug Discov.* 13:140–156. http://dx.doi.org/10.1038/nrd4204

Georgopoulos, K. 2002. Haematopoietic cell-fate decisions, chromatin regulation and ikaros. *Nat. Rev. Immunol.* 2:162–174. http://dx.doi.org/10.1038/nri747

Grover, A., E. Mancini, S. Moore, A.J. Mead, D. Atkinson, K.D. Rasmussen, D. O'Carroll, S.E. Jacobsen, and C. Nerlov. 2014. Erythropoietin guides multipotent hematopoietic progenitor cells toward an erythroid fate. *J. Exp. Med.* 211:181–188. http://dx.doi.org/10.1084/jem.20131189

Hers, I., E.E. Vincent, and J.M. Tavaré. 2011. Akt signalling in health and disease. *Cell. Signal.* 23:1515–1527. http://dx.doi.org/10.1016/j.cellsig.2011.05.004

Inoki, K., J. Kim, and K.L. Guan. 2012. AMPK and mTOR in cellular energy homeostasis and drug targets. *Annu. Rev. Pharmacol. Toxicol.* 52:381–400. http://dx.doi.org/10.1146/annurev-pharmtox-010611-134537

Iwasaki, H., and K. Akashi. 2007. Myeloid lineage commitment from the hematopoietic stem cell. *Immunity.* 26:726–740. http://dx.doi.org/10.1016/j.immuni.2007.06.004

Johnson, S.C., P.S. Rabinovitch, and M. Kaeberlein. 2013. mTOR is a key modulator of ageing and age-related disease. *Nature.* 493:338–345. http://dx.doi.org/10.1038/nature11861

Kfoury, Y., F. Mercier, and D.T. Scadden. 2014. SnapShot: The hematopoietic stem cell niche. *Cell.* 158:228. http://dx.doi.org/10.1016/j.cell.2014.06.019

Khan, M.T., M. Nieuwdorp, and F. Bäckhed. 2014. Microbial modulation of insulin sensitivity. *Cell Metab.* 20:753–760. http://dx.doi.org/10.1016/j.cmet.2014.07.006

Kondo, M. 2010. Lymphoid and myeloid lineage commitment in multipotent hematopoietic progenitors. *Immunol. Rev.* 238:37–46. http://dx.doi.org/10.1111/j.1600-065X.2010.00963.x

Lamming, D.W., L. Ye, P. Katajisto, M.D. Goncalves, M. Saitoh, D.M. Stevens, J.G. Davis, A.B. Salmon, A. Richardson, R.S. Ahima, et al. 2012. Rapamycin-induced insulin resistance is mediated by mTORC2 loss and uncoupled from longevity. *Science.* 335:1638–1643. http://dx.doi.org/10.1126/science.1215135

Laplante, M., and D.M. Sabatini. 2012. mTOR signaling in growth control and disease. *Cell.* 149:274–293. http://dx.doi.org/10.1016/j.cell.2012.03.017

Laurenti, E., S. Doulatov, S. Zandi, I. Plumb, J. Chen, C. April, J.B. Fan, and J.E. Dick. 2013. The transcriptional architecture of early human hematopoiesis identifies multilevel control of lymphoid commitment. *Nat. Immunol.* 14:756–763. http://dx.doi.org/10.1038/ni.2615

Luc, S., K. Anderson, S. Kharazi, N. Buza-Vidas, C. Böiers, C.T. Jensen, Z. Ma, L. Wittmann, and S.E. Jacobsen. 2008. Down-regulation of Mpl marks the transition to lymphoid-primed multipotent progenitors with gradual loss of granulocyte-monocyte potential. *Blood.* 111:3424–3434. http://dx.doi.org/10.1182/blood-2007-08-108324

Mantel, C., S. Messina-Graham, A. Moh, S. Cooper, G. Hangoc, X.Y. Fu, and H.E. Broxmeyer. 2012. Mouse hematopoietic cell-targeted STAT3 deletion: stem/progenitor cell defects, mitochondrial dysfunction, ROS overproduction, and a rapid aging-like phenotype. *Blood.* 120:2589–2599. http://dx.doi.org/10.1182/blood-2012-01-404004

Mendelson, A., and P.S. Frenette. 2014. Hematopoietic stem cell niche maintenance during homeostasis and regeneration. *Nat. Med.* 20:833–846. http://dx.doi.org/10.1038/nm.3647

Méndez-Ferrer, S., D. Lucas, M. Battista, and P.S. Frenette. 2008. Haematopoietic stem cell release is regulated by circadian oscillations. *Nature.* 452:442–447. http://dx.doi.org/10.1038/nature06685

Miller, J.P., and D. Allman. 2005. Linking age-related defects in B lymphopoiesis to the aging of hematopoietic stem cells. *Semin. Immunol.* 17:321–329. http://dx.doi.org/10.1016/j.smim.2005.05.003

Montecino-Rodriguez, E., and K. Dorshkind. 2006. Evolving patterns of lymphopoiesis from embryogenesis through senescence. *Immunity.* 24:659–662. http://dx.doi.org/10.1016/j.immuni.2006.06.001

Morita, Y., H. Ema, and H. Nakauchi. 2010. Heterogeneity and hierarchy within the most primitive hematopoietic stem cell compartment. *J. Exp. Med.* 207:1173–1182. http://dx.doi.org/10.1084/jem.20091318

Morrison, S.J., and D.T. Scadden. 2014. The bone marrow niche for haematopoietic stem cells. *Nature.* 505:327–334. http://dx.doi.org/10.1038/nature12984

Mossadegh-Keller, N., S. Sarrazin, P.K. Kandalla, L. Espinosa, E.R. Stanley, S.L. Nutt, J. Moore, and M.H. Sieweke. 2013. M-CSF instructs myeloid lineage fate in single haematopoietic stem cells. *Nature.* 497:239–243. http://dx.doi.org/10.1038/nature12026

Naik, S.H., L. Perié, E. Swart, C. Gerlach, N. van Rooij, R.J. de Boer, and T.N. Schumacher. 2013. Diverse and heritable lineage imprinting of early haematopoietic progenitors. *Nature.* 496:229–232. http://dx.doi.org/10.1038/nature12013

Nodland, S.E., M.A. Berkowska, A.A. Bajer, N. Shah, D. de Ridder, J.J. van Dongen, T.W. LeBien, and M.C. van Zelm. 2011. IL-7R expression and IL-7 signaling confer a distinct phenotype on developing human B-lineage cells. *Blood.* 118:2116–2127. http://dx.doi.org/10.1182/blood-2010-08-302513

Oguro, H., L. Ding, and S.J. Morrison. 2013. SLAM family markers resolve functionally distinct subpopulations of hematopoietic stem cells and multipotent progenitors. *Cell Stem Cell.* 13:102–116. http://dx.doi.org/10.1016/j.stem.2013.05.014

Otton, R., F.G. Soriano, R. Verlengia, and R. Curi. 2004. Diabetes induces apoptosis in lymphocytes. *J. Endocrinol.* 182:145–156. http://dx.doi.org/10.1677/joe.0.1820145

Powell, J.D., K.N. Pollizzi, E.B. Heikamp, and M.R. Horton. 2012. Regulation of immune responses by mTOR. *Annu. Rev. Immunol.* 30:39–68. http://dx.doi.org/10.1146/annurev-immunol-020711-075024

Quirion, M.R., G.D. Gregory, S.E. Umetsu, S. Winandy, and M.A. Brown. 2009. Cutting edge: Ikaros is a regulator of Th2 cell differentiation. *J. Immunol.* 182:741–745. http://dx.doi.org/10.4049/jimmunol.182.2.741

Raz, R., C.K. Lee, L.A. Cannizzaro, P. d'Eustachio, and D.E. Levy. 1999. Essential role of STAT3 for embryonic stem cell pluripotency. *Proc. Natl. Acad. Sci. USA.* 96:2846–2851. http://dx.doi.org/10.1073/pnas.96.6.2846

Riddell, J., R. Gazit, B.S. Garrison, G. Guo, A. Saadatpour, P.K. Mandal, W. Ebina, P. Volchkov, G.C. Yuan, S.H. Orkin, and D.J. Rossi. 2014. Reprogramming committed murine blood cells to induced hematopoietic stem cells with defined factors. *Cell.* 157:549–564. http://dx.doi.org/10.1016/j.cell.2014.04.006

Rossi, L., K.K. Lin, N.C. Boles, L. Yang, K.Y. King, M. Jeong, A. Mayle, and M.A. Goodell. 2012. Less is more: unveiling the functional core of hematopoietic stem cells through knockout mice. *Cell Stem Cell.* 11:302–317. http://dx.doi.org/10.1016/j.stem.2012.08.006

Samuel, V.T., and G.I. Shulman. 2012. Mechanisms for insulin resistance: common threads and missing links. *Cell.* 148:852–871. http://dx.doi.org/10.1016/j.cell.2012.02.017

Sarbassov, D.D., S.M. Ali, S. Sengupta, J.H. Sheen, P.P. Hsu, A.F. Bagley, A.L. Markhard, and D.M. Sabatini. 2006. Prolonged rapamycin treatment inhibits mTORC2 assembly and Akt/PKB. *Mol. Cell.* 22:159–168. http://dx.doi.org/10.1016/j.molcel.2006.03.029

Schepers, K., T.B. Campbell, and E. Passegué. 2015. Normal and leukemic stem cell niches: insights and therapeutic opportunities. *Cell Stem Cell.* 16:254–267. http://dx.doi.org/10.1016/j.stem.2015.02.014

Shim, J., T. Mukherjee, and U. Banerjee. 2012. Direct sensing of systemic and nutritional signals by haematopoietic progenitors in Drosophila. *Nat. Cell Biol.* 14:394–400. http://dx.doi.org/10.1038/ncb2453

Shimobayashi, M., and M.N. Hall. 2014. Making new contacts: the mTOR network in metabolism and signalling crosstalk. *Nat. Rev. Mol. Cell Biol.* 15:155–162. http://dx.doi.org/10.1038/nrm3757

Singer, K., J. DelProposto, D.L. Morris, B. Zamarron, T. Mergian, N. Maley, K.W. Cho, L. Geletka, P. Subbaiah, L. Muir, et al. 2014. Diet-induced obesity promotes myelopoiesis in hematopoietic stem cells. *Mol. Metab.* 3:664–675. http://dx.doi.org/10.1016/j.molmet.2014.06.005

Taguchi, A., and M.F. White. 2008. Insulin-like signaling, nutrient homeostasis, and life span. *Annu. Rev. Physiol.* 70:191–212. http://dx.doi.org/10.1146/annurev.physiol.70.113006.100533

Takeda, K., B.E. Clausen, T. Kaisho, T. Tsujimura, N. Terada, I. Förster, and S. Akira. 1999. Enhanced Th1 activity and development of chronic enterocolitis in mice devoid of Stat3 in macrophages and neutrophils. *Immunity.* 10:39–49. http://dx.doi.org/10.1016/S1074-7613(00)80005-9

Tamplin, O.J., E.M. Durand, L.A. Carr, S.J. Childs, E.J. Hagedorn, P. Li, A.D. Yzaguirre, N.A. Speck, and L.I. Zon. 2015. Hematopoietic stem cell arrival triggers dynamic remodeling of the perivascular niche. *Cell.* 160:241–252. http://dx.doi.org/10.1016/j.cell.2014.12.032

Uhmann, A., K. Dittmann, F. Nitzki, R. Dressel, M. Koleva, A. Frommhold, A. Zibat, C. Binder, I. Adham, M. Nitsche, et al. 2007. The Hedgehog receptor Patched controls lymphoid lineage commitment. *Blood.* 110:1814–1823. http://dx.doi.org/10.1182/blood-2007-02-075648

Urban, J.A., and S. Winandy. 2004. Ikaros null mice display defects in T cell selection and CD4 versus CD8 lineage decisions. *J. Immunol.* 173:4470–4478. http://dx.doi.org/10.4049/jimmunol.173.7.4470

Walter, D., A. Lier, A. Geiselhart, F.B. Thalheimer, S. Huntscha, M.C. Sobotta, B. Moehrle, D. Brocks, I. Bayindir, P. Kaschutnig, et al. 2015. Exit from dormancy provokes DNA-damage-induced attrition in haematopoietic stem cells. *Nature.* 520:549–552. http://dx.doi.org/10.1038/nature14131

Wang, S., P. Xia, B. Ye, G. Huang, J. Liu, and Z. Fan. 2013. Transient activation of autophagy via Sox2-mediated suppression of mTOR is an important early step in reprogramming to pluripotency. *Cell Stem Cell.* 13:617–625. http://dx.doi.org/10.1016/j.stem.2013.10.005

Wen, Z., Z. Zhong, and J.E. Darnell Jr. 1995. Maximal activation of transcription by Stat1 and Stat3 requires both tyrosine and serine phosphorylation. *Cell.* 82:241–250. http://dx.doi.org/10.1016/0092-8674(95)90311-9

Will, B., T.O. Vogler, B. Bartholdy, F. Garrett-Bakelman, J. Mayer, L. Barreyro, A. Pandolfi, T.I. Todorova, U.C. Okoye-Okafor, R.F. Stanley, et al. 2013. Satb1 regulates the self-renewal of hematopoietic stem cells by promoting quiescence and repressing differentiation commitment. *Nat. Immunol.* 14:437–445. http://dx.doi.org/10.1038/ni.2572

Xia, P., S. Wang, Y. Du, Z. Zhao, L. Shi, L. Sun, G. Huang, B. Ye, C. Li, Z. Dai, et al. 2013. WASH inhibits autophagy through suppression of Beclin 1 ubiquitination. *EMBO J.* 32:2685–2696. http://dx.doi.org/10.1038/emboj.2013.189

Xia, P., S. Wang, G. Huang, P. Zhu, M. Li, B. Ye, Y. Du, and Z. Fan. 2014. WASH is required for the differentiation commitment of hematopoietic stem cells in a c-Myc-dependent manner. *J. Exp. Med.* 211:2119–2134. http://dx.doi.org/10.1084/jem.20140169

Xia, P., S. Wang, Z. Xiong, B. Ye, L.-Y. Huang, Z.-G. Han, and Z. Fan. 2015a. IRTKS negatively regulates antiviral immunity through PCBP2 sumoylation-mediated MAVS degradation. *Nat. Commun.* 6:8132. http://dx.doi.org/10.1038/ncomms9132

Xia, P., S. Wang, B. Ye, Y. Du, G. Huang, P. Zhu, and Z. Fan. 2015b. Sox2 functions as a sequence-specific DNA sensor in neutrophils to initiate innate immunity against microbial infection. *Nat. Immunol.* 16:366–375. http://dx.doi.org/10.1038/ni.3117

Yan, X., J. Chen, C. Zhang, S. Zhou, Z. Zhang, J. Chen, W. Feng, X. Li, and Y. Tan. 2015. FGF21 deletion exacerbates diabetic cardiomyopathy by aggravating cardiac lipid accumulation. *J. Cell. Mol. Med.* 19:1557–1568. http://dx.doi.org/10.1111/jcmm.12530

Yip, C.K., K. Murata, T. Walz, D.M. Sabatini, and S.A. Kang. 2010. Structure of the human mTOR complex I and its implications for rapamycin inhibition. *Mol. Cell.* 38:768–774. http://dx.doi.org/10.1016/j.molcel.2010.05.017

Yoshida, T., S.Y. Ng, J.C. Zuniga-Pflucker, and K. Georgopoulos. 2006. Early hematopoietic lineage restrictions directed by Ikaros. *Nat. Immunol.* 7:382–391. http://dx.doi.org/10.1038/ni1314

Yu, H., H. Lee, A. Herrmann, R. Buettner, and R. Jove. 2014. Revisiting STAT3 signalling in cancer: new and unexpected biological functions. *Nat. Rev. Cancer.* 14:736–746. http://dx.doi.org/10.1038/nrc3818

Yu, L., C.K. McPhee, L. Zheng, G.A. Mardones, Y. Rong, J. Peng, N. Mi, Y. Zhao, Z. Liu, F. Wan, et al. 2010. Termination of autophagy and reformation of lysosomes regulated by mTOR. *Nature.* 465:942–946. http://dx.doi.org/10.1038/nature09076